Atmos. Chem. Phys. Discuss., doi:10.5194/acp-2016-1123, 2017
Manuscript under review for journal Atmos. Chem. Phys.
Published: 16 January 2017

Atmospheric Chemistry and Physics Discussions

Observation- and Model-Based Estimates of Particulate Dry Nitrogen Deposition to the Oceans

Alex R. Baker [1], Maria Kanakidou [2], Katye E. Altieri [3], Nikos Daskalakis [2,15], Gregory S. Okin [4], Stelios Myriokefalitakis [2,16], Frank Dentener [5], Mitsuo Uematsu [6], Manmohan M. Sarin [7], Robert A. Duce [8], James N. Galloway [9], William C. Keene [9], Arvind Singh [7], Lauren Zamora [10,11], Jean-Francois Lamarque [12], Shih-Chieh Hsu [13*], Shital S. Rohekar [1,17], Joseph M. Prospero [14]

[1]Centre for Ocean and Atmospheric Science, School of Environmental Sciences, University of East Anglia, Norwich NR4 7TJ, UK
[2]Environmental Chemical Processes Laboratory, Department of Chemistry, University of Crete, PO Box 2208, Heraklion 7, Greece
[3]Energy Research Centre, University of Cape Town, South Africa.
[4]Department of Geography, University of California at Los Angeles, California, USA
[5]European Commission, Joint Research Centre, Ispra, Italy
[6]Center for International Collaboration, Atmosphere and Ocean Research Institute, The University of Tokyo, Chiba, Japan
[7]Geosciences Division, Physical Research Laboratory, Ahmedabad, 380009, India
[8]Departments of Oceanography and Atmospheric Sciences, Texas A&M University, College Station, Texas, USA
[9]Department of Environmental Sciences, University of Virginia, Charlottesville, Virginia, USA
[10]Climate and Radiation Laboratory, NASA Goddard Space Flight Center, Greenbelt, MD, USA
[11]Universities Space Research Association, Columbia, MD, USA
[12]NCAR Earth System Laboratory, National Center for Atmospheric Research, Boulder, CO, USA
[13]Research Center for Environmental Changes, Academia Sinica, Nankang, Taipei, Taiwan
[14]Rosenstiel School of Marine and Atmospheric Sciences, University of Miami, Miami, Florida, USA
[15]now at LATMOS/IPSL, UPMC Univ. Paris 06 Sorbonne Universités, UVSQ, CNRS, Paris, France
[16]now at IMAU, University of Utrecht, 3584 CC Utrecht, Netherlands
[17]now at School of Physics, Astronomy and Maths, University of Hertfordshire, Hatfield, UK
* Deceased 10th October 2014

Correspondence to: Alex R. Baker (alex.baker@uea.ac.uk)

Atmos. Chem. Phys. Discuss., doi:10.5194/acp-2016-1123, 2017
Manuscript under review for journal Atmos. Chem. Phys.
Published: 16 January 2017

Atmospheric Chemistry and Physics Discussions

Abstract

Nitrogen (N) emissions to the atmosphere have increased by a factor of 3-4 through anthropogenic activity since the Industrial Revolution. This has led to large increases in the deposition of nitrate (NO_3^-) and ammonium (NH_4^+) to the surface waters of the open ocean, with potential impacts on marine productivity and the global carbon cycle. Global-scale understanding of N deposition to the oceans is reliant on our ability to produce and validate models of nitrogen emission, atmospheric chemistry, transport and deposition. In this work, ~2900 observations of aerosol NO_3^- and NH_4^+ concentrations, acquired from sampling aboard ships in the period 1995 - 2012, are used to assess the performance of modelled N concentration and deposition fields over the remote ocean. Three ocean regions (the eastern tropical North Atlantic, the northern Indian Ocean and northwest Pacific) were selected in which the density and distribution of observational data were considered sufficient to provide effective comparison to model products. All of these study regions are affected by transport and deposition of mineral dust, which alters the deposition of N.

Surface particulate NO_3^- and NH_4^+ concentrations simulated by the TM4-ECPL (TM4) model were compared to observed aerosol concentrations. Dry deposition fluxes of these species predicted by TM4 (ModDep) were compared with equivalent fluxes calculated from the observed concentrations (CalDep) using two commonly applied methods for the determination of CalDep. CalDep was also compared to total dry deposition fluxes of oxidised N (NO_y) and reduced N (NH_x) from TM4 and the ACCMIP multi-model mean product. Comparison in the three study regions suggests that TM4 over-estimates NO_3^- concentrations and under-estimates NH_4^+ concentrations, with spatial distributions in the tropical Atlantic and northern Indian Ocean not being reproduced by the model. In the case of NH_4^+ in the Indian Ocean, this discrepancy was probably due to seasonal biases in the sampling. Similar patterns were observed in the various comparisons of CalDep to ModDep and it was not possible to assess objectively the relative merits of the two methods for estimating CalDep. Comparisons of NH_4^+ CalDep to NH_x ModDep were impaired by the significant fraction of gas-phase NH_3 deposition incorporated in the TM4 and ACCMIP model products. All of the comparisons (of concentration and deposition) suffered due to the large uncertainty in dry deposition velocities used in the models and in the calculation of CalDep. These uncertainties have been a major limitation on estimates of the flux of material to the oceans for several decades.

Atmos. Chem. Phys. Discuss., doi:10.5194/acp-2016-1123, 2017
Manuscript under review for journal Atmos. Chem. Phys.
Published: 16 January 2017

Atmospheric Chemistry and Physics Discussions

1 Introduction

Global emissions of inorganic nitrogen (i.e. all nitrogen (N) species, excluding N_2) to the atmosphere have likely increased by factors of 3-4 since the onset of industrialisation in the mid-nineteenth century (Duce et al., 2008; Galloway et al., 2008). Major sources include the emission of nitrogen oxides (NO_x) as a by-product of combustion (Galloway et al., 2004) and ammonia (NH_3) emissions resulting from fertilizer application and intensive livestock-rearing practices (Bouwman et al., 1997). On-going implementation of emission controls (mostly affecting NO_x) and global economic development will lead to further changes in both the magnitude and spatial distribution of nitrogen emissions over the coming decades (e.g. Dentener et al., 2006; Lamarque et al., 2013a).

Nitrogen deposition impacts both terrestrial and marine ecosystems. N is a limiting nutrient for primary producers over ~70% of the global ocean (Duce et al., 2008). Its deposition enhances primary productivity in low-nitrogen marine ecosystems (e.g. Zamora et al., 2010; Singh et al., 2012) and potentially drives ecological shifts through changes in nutrient regimes (Kim et al., 2011; Chung et al., 2011; Shi et al., 2012; Mourino-Carballido et al., 2012; Chien et al., 2016). Export of atmospheric N into sub-oxic or anoxic zones of, for example, the Arabian Sea will lead to non-linear effects on the marine and atmospheric N cycle through the processes of denitrification and N_2O production and consumption (Suntharalingam et al., 2012; Landolfi et al., 2013; Somes et al., 2016).

In order for these impacts to be understood, it is necessary to quantify the deposition of nitrogen species from the atmosphere. At a local scale this can be achieved through sustained observations of nitrogen species concentrations in deposition, and in a very few terrestrial cases (North America, western Europe and East Asia) networks of observational stations have been established that allow N deposition to be monitored on regional scales. Outside of these regions, and especially over the oceans, large-scale assessment of atmospheric N deposition is almost exclusively achieved through the use of global atmospheric chemical-transport modelling.

The utility of these models (both for estimating current N deposition and in predicting future deposition rates) is dependent on their skill in replicating many complex parameters, including nitrogen species' emission rates and distributions, chemical interactions, transport pathways and deposition mechanisms. A number of such models have been inter-compared as part of the Atmospheric Chemistry and Climate Model Intercomparison Project, ACCMIP (Lamarque et al., 2013b), and modelled deposition fields have been used in a number of studies (e.g. Lamarque et al., 2013a). ACCMIP produced multi-model mean (MMM) estimates of both oxidised (NO_y) and reduced (NH_x) inorganic N deposition for the present-day due to both dry and wet deposition. The skill of these ACCMIP MMM deposition estimates was assessed principally by comparison against the North American, European and East Asia wet deposition networks on land (see Lamarque et al., 2013a) using a benchmark dataset described in Vet et al. (2014).

Atmos. Chem. Phys. Discuss., doi:10.5194/acp-2016-1123, 2017
Manuscript under review for journal Atmos. Chem. Phys.
Published: 16 January 2017

Atmospheric Chemistry and Physics Discussions

Deposition monitoring does occur at some remote marine locations (e.g. Mace Head, Ireland, Bermuda, Barbados, Amsterdam Island (Keene et al., 2015)), but it is impractical to establish deposition networks over wide areas of the open ocean, due to the limitations of suitable sites and the challenges of maintaining rigorous sampling programmes at such remote locations. Thus, assessment of the impacts of atmospheric N deposition on oceanic processes, including primary production, CO_2 uptake, and species diversity, has so far been reliant on the fidelity of deposition models that have not been validated for the oceans.

In this work, the abilities of the ACCMIP MMM (Lamarque et al., 2013a) and the TM4-ECPL model, hereafter TM4 (Kanakidou et al., 2016; Myriokefalitakis et al., 2015), to estimate atmospheric N dry deposition to the ocean are evaluated. The evaluation was done by comparison to a substantial database of aerosol N observations collected during ships' voyages over all the major ocean basins. Similar evaluations of dry deposition of organic N and wet deposition of inorganic N were not possible because there was very little observational data available over the oceans in these cases. This manuscript describes the database of aerosol N species (nitrate, NO_3^- and ammonium, NH_4^+) concentrations that was assembled and the results of comparing this database to the models at the global scale, as well as in three specific regions: the tropical eastern Atlantic (TEAtl), the northern Indian Ocean (NInd) and the margins of the Northwest Pacific (NWPac).

2 Methods

2.1 The aerosol nitrate and ammonium concentration database

Aerosol NO_3^- and NH_4^+ concentration data were acquired for 2890 samples collected from >120 ship-based studies over the period 1995 – 2012. The spatial distributions of these samples is shown in Fig. 1a and a description of the individual cruises, the data sources and contributors is given in the supplementary material for this manuscript (Table S1). The database itself (aerosol concentrations and sample locations) is also available in the supplementary material. In general, the data were accessed from publicly available data archives (i.e. the SOLAS aerosol and rain chemistry database (http://www.bodc.ac.uk/solas_integration/implementation_products/group1/aerosol_rain/), the NOAA-PMEL Atmospheric Chemistry Data Server (http://saga.pmel.noaa.gov/data/)), were provided directly by the originator or were unpublished results from the authors. Since the data originate from multiple sources, the samples were acquired using a variety of sampling devices (e.g. bulk filtration or in size fractions using cascade impactors) and collection substrates (e.g. Whatman 41, glass fibre or quartz) and were analysed using different techniques (commonly ion chromatography or automated spectrophotometry) in many different laboratories. Thus the presence of biases within the database cannot be ruled out. In cases where the observations were obtained for multiple size fractions for a given sample, the fraction concentrations were summed and stored in the database only as total NO_3^- or NH_4^+ concentrations for that sample.

The database contains ~1420, ~680 and ~770 samples collected over the Atlantic, Indian and Pacific Oceans respectively. Overall, 81% of the samples contain observations of both NO_3^- and NH_4^+, 16% observations of NO_3^- alone and 3% of NH_4^+

Atmos. Chem. Phys. Discuss., doi:10.5194/acp-2016-1123, 2017
Manuscript under review for journal Atmos. Chem. Phys.
Published: 16 January 2017

alone. The distributions of these samples are non-uniform with time (by year and by month) through the 16-year period that we examined, as illustrated for the major ocean basins in Fig. 1b & c.

2.2 Parameters to be compared to model output

Where possible, the observed aerosol concentrations (C) for NO_3^- and NH_4^+ were compared directly with corresponding particulate concentrations simulated by the models (i.e. for the TM4 model, see below). Dry deposition fluxes from the models were also compared to the observational database. In order to do so, dry deposition fluxes (F) were calculated from the observed concentrations of the two species using dry deposition velocities (v_d) (Eq. 1).

$$F = v_d C \quad (1)$$

Two approaches were used to the calculation of F. In one case, fixed values for v_d of 0.9 cm s^{-1} for NO_3^- and 0.1 cm s^{-1} for NH_4^+ were used to calculate F in all grid cells (hereafter referred to as the "fixed v_d" method). For NO_3^-, the relatively high v_d value used reflects its associated over the ocean with coarse sea-salt particles (and is similar to the v_d for gaseous HNO_3). The lower v_d value of NH_4^+ is due to its association fine aerosol fractions. Similar methods have been applied to the calculation of dry deposition fluxes in many previous studies (e.g. Markaki et al., 2003; Buck et al., 2013; Baker et al., 2016). Dry deposition fluxes were also calculated using wind speed-dependent values of v_d (Ganzeveld et al., 1998), calculated for each grid cell using ECMWF Interim reanalysis dataset surface wind speed, for particles of 7 µm (coarse mode) and 0.6 µm (fine mode) diameter, as done by Baker et al. (2010) and Powell et al. (2015) – the "variable v_d" method. In this case, the total NO_3^- and NH_4^+ concentrations in the database were artificially separated into coarse and fine modes using the median fractions of each species in coarse mode aerosol reported for 210 aerosol samples collected over the Atlantic Ocean (Baker et al., 2010). These fractions were 0.90 and 0.14 for NO_3^- and NH_4^+ respectively. (For comparison, in TM4 on a global scale, these fractions were 0.92 and 0.08 respectively for the year 2005). The mean values of v_d for NO_3^- and NH_4^+ calculated using the variable method over the global ocean were 0.81 cm s^{-1} and 0.15 cm s^{-1} respectively and their distribution is shown in Fig. S1 of the Supplementary Material. Hereafter, deposition fluxes derived from measured aerosol concentrations and dry deposition velocities are referred to as "Calculated Deposition (CalDep)".

2.3 Model products

For the TM4 model, surface level particulate NO_3^- and NH_4^+ concentrations and dry deposition fluxes of these species were simulated for the nominal year 2005 (for details see Kanakidou et al., 2016; Myriokefalitakis et al., 2015). The model's native resolution is 2° (lat.) x 3° (lon.), but for this study the model output was interpolated to a grid scale of 1° x 1°. The TM4 model also applies the Ganzeveld et al. (1998) parameterisation to compute v_d for each grid cell using ECMWF ERA interim meteorology for the year 2005 (see Kanakidou et al., 2012). TM4 also assumes dry mass diameters of 0.34 µm (sigma 1.59) and 6.71 µm (sigma 2.00) for sea-salt aerosol and 0.68 µm (sigma 1.59) and 3.5 µm (sigma 2.00) for dust aerosol that are in

Atmos. Chem. Phys. Discuss., doi:10.5194/acp-2016-1123, 2017
Manuscript under review for journal Atmos. Chem. Phys.
Published: 16 January 2017

Atmospheric Chemistry and Physics Discussions

agreement with those used here to calculate dry deposition based on measured aerosol concentrations. Furthermore, TM4 accounts for 8.15 Tg-N yr^{-1} of NH_3 emissions from the ocean to the atmosphere, taken from the Bouwman et al. (1997) emission inventory and are used in the model based on annual mean fluxes. Although this reduced nitrogen is of marine origin and thus does not constitute an external source of N to the ocean, its consideration is needed when comparing to atmospheric aerosol observations in the marine environment. TM4 also accounts for marine emissions of amines as discussed in Kanakidou et al. (2016). The present TM4 model configuration explicitly considers the atmospheric iron cycle (Myriokefalitakis et al., 2015) and uses the ISORROPIA II thermodynamic equilibrium module (Fountoukis and Nenes, 2007) to calculate the partitioning of NH_3/NH_4^+ and HNO_3/NO_3^- accounting for the impact of sea-salt and dust elements on this partitioning (Myriokefalitakis et al., 2015) assuming stable conditions (Karydis et al., 2016).

The ACCMIP products used in this comparison were based on emissions for the year 2000 and average meteorology for the decade 2000 – 2009 (Lamarque et al., 2013a). The fields used were MMM dry deposition from 10 (for NO_y) or 5 (for NH_x) individual atmospheric chemical-transport models and were reported by ACCMIP on a grid scale of 0.5° x 0.5°, although the resolution of individual models was coarser. NO_y and NH_x dry deposition estimates were also available for TM4. (Neither particulate concentration nor dry deposition fields were available for NO_3^- or NH_4^+ from ACCMIP). For both ACCMIP and TM4 model results, NH_x corresponds to the sum of NH_3 and NH_4^+. However, NO_y differs between the two model products. NO_y is derived from TM4 results as the sum of all inorganic oxidized N species in the model, i.e. NO, NO_2, NO_3^-, N_2O_5, HONO, HNO_4 and HNO_3 (Kanakidou et al., 2016), since organic oxidized N is explicitly studied (Kanakidou et al., 2012). For the ACCMIP models, NO_y also contains some gas-phase organic nitrates and peroxyacyl nitrates (PAN) (Lamarque et al., 2013a). Thus the NO_y and NH_x deposition estimates from both models include contributions from gas-phase, as well as particulate, deposition. (On a global scale, TM4 simulates that particulate NO_3^- and NH_4^+ account for 80% and 35% of inorganic NO_y and NH_x deposition, respectively, while particulate NH_4^+ deposition comprises ~25% of NH_x deposition in the ACCMIP MMM (Lamarque et al., 2013a). Note that these global numbers are dominated by deposition over continents, where particulate NH_4NO_3 is a much more significant component of aerosol N than over the oceans). Modelled NO_y and NH_x deposition estimates are therefore not directly comparable to the observationally-derived deposition estimates examined here. For information, Table S2 presents the total annual emissions of NO_x and NH_3 (and their emissions from Africa, India and southeast Asia / Japan) used by the ACCMIP models and by TM4 for the present study.

Dry deposition fluxes simulated by the TM4 and ACCMIP model products are referred to below as "Modelled Deposition (ModDep)".

2.4 Comparison methods

Observations and model products were compared using a 5° x 5° grid. This represents a compromise between the desire to undertake the comparison at a high spatial resolution and the need to ensure that the amount of observational data available in each grid cell was sufficient to adequately represent the deposition in that cell.

Atmos. Chem. Phys. Discuss., doi:10.5194/acp-2016-1123, 2017
Manuscript under review for journal Atmos. Chem. Phys.
Published: 16 January 2017

Atmospheric Chemistry and Physics Discussions

For the observations, means of all available NO_3^- and NH_4^+ concentrations were calculated for each grid cell. Values of CalDep for each species were then calculated from these mean concentrations using the methods described above. Annual mean model products were prepared for comparison by removing outputs from grid cells that contained land using a (0.5° x 0.5° or 1° x 1°, as appropriate) land-mass mask. This was done in order to prevent high deposition fluxes of N species over land biasing the comparison to the marine observations for grid cells along continental margins. The model outputs were then averaged from their input resolution to the same 5° x 5° grid that was used to bin the observational data.

The following parameters were then compared: observed aerosol concentrations of NO_3^- and NH_4^+ with their simulated concentrations from TM4; CalDep for NO_3^- and NH_4^+ with their respective ModDep from TM4 and with ModDep of NO_y and NH_x from ACCMIP and TM4. Comparisons over regions larger than individual grid cells were made using the area- and sample number-averaged ratio ($R_{A,n}$) of modelled to observation-based parameter (concentration or deposition flux), as shown in Eq. 2, and normalised mean bias (NMB; Eq. 3) (where M is the modelled concentration or ModDep, O is the observed concentration or CalDep, A is the surface area and n is the number of observations for each grid cell).

$$R_{A,n} = \frac{\sum(M/O)\,A\,n}{\sum A\,n} \quad (2)$$

$$NMB = 100\,\frac{\sum(M-O)}{\sum O} \quad (3)$$

Thus the value of $R_{A,n}$ would be equal to unity in the ideal case of perfect agreement between the model annual average and observations in the region in question. When the model deviates from observations, the ratio reflects the model to measurements agreement, favouring the gird cells where most measurements exist compared to the grid cell areas with fewer measurements. Ratios larger than unity indicate over-estimate of observations and lower than unity an under-estimate of the observations.

3 Results

3.1 Observational Database

While the database contains observations that cover wide regions of the global ocean (Fig. 1), for NO_3^- only 550 grid cells (~28% of oceanic grids cells) contain observations. Of those grid cells containing observations, only 65 contained 10 or more NO_3^- observations, and 72 contained observational data acquired over 4 or more calendar months. For NH_4^+, there were observations in 478 grid cells (~24% of oceanic cells), with 57 of those containing 10 or more observations, and 50 with observations acquired over 4 or more months (Table 1). Summaries of the data available for each grid cell over the global ocean (numbers of observations, number of calendar months with observations, mean and relative standard deviation aerosol concentrations) are shown in Fig. S2 and S3 for NO_3^- and NH_4^+ respectively.

Atmos. Chem. Phys. Discuss., doi:10.5194/acp-2016-1123, 2017
Manuscript under review for journal Atmos. Chem. Phys.
Published: 16 January 2017

Atmospheric Chemistry and Physics Discussions

In the following, the global dataset was retained, but detailed analysis focused on the TEAtl, NInd and NWPac study regions (the number of NO_3^- or NH_4^+ observations in each cell and the number of calendar months represented by those observations for these regions are shown in Fig. 9 – 14). Data coverage was best in the TEAtl region (Fig. 2a), where many grid cells had both relatively large numbers of observations and observations covering 6 or more months of a calendar year. In the NInd region (Fig. 2b), there were several grid cells containing many observations, but only one grid cell with observations spanning more than 6 months. Data coverage in most of the NWPac region (Fig. 2c) was poor compared to the other two regions, with high sample numbers and relatively good temporal coverage only in cells close to the coast of China. The NWPac region had the additional benefit that it is adjacent to the Acid Deposition Monitoring Network in East Asia (EANET) that has already been used to assess the skill of the ACCMIP and TM4 modelled wet deposition products (Lamarque et al., 2013a; Kanakidou et al., 2016). The observational data available in these three regions were considered most likely to be representative of the annual N concentration and deposition fields represented by the models, although even here it is apparent that the distribution of observations is non-uniform in and between individual grid cells (Fig. 2). Where possible, the ship-based observations were compared to longer-term records obtained at remote island sites located in specific grid cells (see Sect. 3.2). Where observation – model comparisons are reported outside of those regions (i.e. for the global database) this is on the understanding that these comparisons are likely to be rather uncertain.

3.2 Comparison to Concentrations at Island Monitoring Stations

Figure 3 shows box and whisker plots of NO_3^- and NH_4^+ concentrations grouped according to calendar month for cells containing relatively high numbers (16 – 73) of observations for each of the TEAtl, NInd and NWPac study regions. For two of these cells the monthly and annual mean concentrations are directly compared to observations from remote island monitoring sites situated within those cells (see below). Similar independent records have not been identified in any other grid cell that also contains high numbers of observations in the database.

In the TEAtl region, the data obtained for the 15°-20°N, 25°-20°W cell were compared to results reported for the Cape Verde Atmospheric Observatory (CVAO: 16°51'49" N, 24°52'02" W) for the years 2007-2011 (Fomba et al., 2014). Here agreement between the ship-based observations and the island station was rather good for NO_3^-, with the range of the 42 ship-based concentrations falling entirely within the range of the 671 observations at CVAO (Fig. 3a). The mean NO_3^- concentration for the ship observations was 20.7 nmol m^{-3}, compared to the 5-year mean concentration of 17.7 nmol m^{-3} for the island observations, with neither dataset showing significant seasonal variation. There was also generally good agreement between the ship and island observations of ammonium in this cell, with the exception of July, where the ship data (2 samples) were approximately a factor of 2 higher than the upper limit of the island data (Fig. 3g). Mean NH_4^+ concentrations were 13.9 nmol m^{-3} for the ship observations (n = 35) and 5.0 nmol m^{-3} (5-year average) for the island observations. Fomba et al. (2014) reported a small seasonal cycle for NH_4^+ at CVAO, with higher concentrations during March – June than during the rest of the year. There was not enough ship data available to independently confirm this seasonal pattern.

Atmos. Chem. Phys. Discuss., doi:10.5194/acp-2016-1123, 2017
Manuscript under review for journal Atmos. Chem. Phys.
Published: 16 January 2017

In the NWPac region, there was also good agreement between the 73 ship-based observations from 2005 - 2008 in the 25°-30°N, 120°-125°E cell and the 173 daily observations made during 2010 at Pengchiayu Island (25°37'44" N, 122°4'4" E) in the East China Sea (Hsu et al., 2014). The Pengchiayu dataset indicated that there was some seasonality in aerosol NO_3^- concentrations at this site (Fig. 3e), with mean concentration values being approximately twice as high during the months of December to April, than during May to October. Mean NO_3^- concentrations were 67.8 nmol m^{-3} for the ship-based observations and 71.0 nmol m^{-3} at Pengchiayu Island. Except for January and September, there was little monthly variation in NH_4^+ concentrations at Pengchiayu (Fig. 3k). Mean NH_4^+ concentrations were 88.7 nmol m^{-3} and 91.4 nmol m^{-3} for the ship and island observations respectively.

3.3 Comparison of Observed and Modelled Concentrations

Comparisons of observed aerosol concentrations for NO_3^- and NH_4^+ with modelled surface level particulate concentrations from TM4 for these species are shown in Fig. 4. The sample number weighting included in the calculation of $R_{A,n}$ is illustrated in Fig. 4 using crosses of different sizes to represent the amount of data available in each cell.

For NO_3^-, TM4 generally over-estimated aerosol concentrations ($R_{A,n}$ = 6.6 for the global dataset), although the model appears to significantly under-estimate NO_3^- concentrations in the Atlantic sector of the Southern Ocean (see Fig. S4a: note that there was relatively little observational data in this region). Over-estimation of aerosol NO_3^- concentrations was particularly noticeable over the Bay of Bengal, the northwest Pacific around Japan and for some areas of the northwest Atlantic, including for a number of coastal grid cells around North America that contained relatively large numbers of observations (Fig. 4a). Spatial gradients in aerosol concentrations over coastal areas are likely to be strong and this may contribute to the large observation – model discrepancies for these grid cells. For the TEAtl region, TM4 reproduced the regional average aerosol NO_3^- concentration better than was the case for the global comparison ($R_{A,n}$ = 1.4). However, TM4 did not reproduce the spatial distribution of NO_3^- in this region, particularly around the margins of West Africa (Fig. 5). Regional concentration over-estimates by TM4 in the NInd ($R_{A,n}$ = 2.9) and NWPac ($R_{A,n}$ = 2.6) regions appear to be due to over-estimation over the Arabian Sea and Bay of Bengal and the seas around Korea and Japan respectively (Fig. 5).

Over the global dataset, agreement between the observations and TM4 concentrations was better for NH_4^+ than for NO_3^- ($R_{A,n}$ = 0.9, indicating a slight model under-estimation). However, under-estimation of NH_4^+ concentrations by TM4 was greater in all of the three study regions and the global value of $R_{A,n}$ appears to be influenced by model over-estimation in regions with low observed NH_4^+ concentrations (Fig. 4b). Specifically, TM4 appears to over-estimate NH_4^+ concentrations in the western South Atlantic and equatorial Pacific Oceans, while under-estimation occurred in the NWPac region and southeastern South Atlantic (Fig. S4b). Although TM4 appeared to under-estimate NH_4^+ concentrations across the TEAtl ($R_{A,n}$ = 0.7) and NWPac ($R_{A,n}$ = 0.5) regions, the spatial distributions of NH_4^+ in the observations and model were similar (Fig. 6). In the NInd region ($R_{A,n}$ = 0.7), TM4 did not appear to reproduce the spatial distribution of NH_4^+, with observed concentrations in the Bay of Bengal and in the cells around 5°S - 10°N, 65° - 80°E being higher than those simulated by the model.

Atmos. Chem. Phys. Discuss., doi:10.5194/acp-2016-1123, 2017
Manuscript under review for journal Atmos. Chem. Phys.
Published: 16 January 2017

Atmospheric Chemistry and Physics Discussions

3.4 Comparison of Dry Deposition Estimates

Figure 7 shows the comparison between CalDep from the variable v_d method for NO_3^- and NH_4^+ and ModDep of NO_y / NO_3^- and NH_x / NH_4^+ from the models for all grid cells which contained observations. (A similar figure for CalDep from the fixed v_d method is shown in Fig S5).

The comparison to NO_3^- CalDep for the global oceanic dataset indicates that the models generally over-estimated the flux (Table 2), with values of $R_{A,n}$ of at least 4 in all cases (Figs. 7 & S5). The ACCMIP simulation appeared to over-estimate NO_y deposition in the northern hemisphere and under-estimate in the southern hemisphere, while TM4 showed a less pronounced difference in performance between the northern and the southern hemisphere with over- and under-estimates in both hemispheres and a clear under-estimate in NO_y / NO_3^- deposition over the Southern Ocean (Fig. S6). Values of $R_{A,n}$ for the global TM4 deposition comparison (4.4 – 5.6) were all slightly lower than that for the TM4 concentration comparison (6.6). This must be due to differences between the average dry deposition velocity used for NO_y / NO_3^-, which is lower in TM4 than in either CalDep method. For NO_3^-, the use of the variable v_d CalDep method led to lower observation-based deposition fluxes and higher values of $R_{A,n}$ (i.e. generally worse overall agreement to the models), when compared to the fixed v_d method. This indicates that the average deposition velocity for NO_y / NO_3^- used by the models was closer to the value used in the fixed v_d case (0.9 cm s^{-1}) than to the average deposition velocity used in the variable v_d case, but does not necessarily imply that the models or fixed v_d case are more accurate representations of aerosol nitrate dry deposition. For TM4, values of $R_{A,n}$ were generally closer to unity for simulated NO_3^- than for NO_y (i.e. agreement was better when the simulation more closely matched the measured parameter).

For NH_4^+, the global comparison (Figs. 7 & S5) indicates that the modelled NH_x deposition results were considerably higher than NH_4^+ CalDep ($R_{A,n}$ = 3.0 – 5.4). This is primarily due to the large component of gas-phase NH_3 deposition in the modelled NH_x fluxes (for ACCMIP NH_x : NH_4^+ = ~4 (Lamarque et al., 2013a), while in TM4 this ratio is ~2.5). The greatest disagreement between NH_x ModDep and CalDep was at the lowest NH_4^+ deposition fluxes (<0.01 mg N m^{-2} d^{-1}), which were over-estimated in the models by 1 – 2 orders of magnitude, generally over the tropical open oceans (Fig. S7). This mismatch between NH_4^+ CalDep and NH_x ModDep makes meaningful comparison between these fields rather difficult. Therefore NH_4^+ CalDep - NH_x ModDep comparisons for the three study regions are not discussed below. TM4 NH_4^+ ModDep fluxes agreed better (in the global comparison) with the corresponding CalDep fluxes ($R_{A,n}$ = 1.1 – 1.4, Figs. 7f &S5f) than the NH_x ModDep results. Use of the variable v_d method led to higher CalDep fluxes for NH_4^+ and hence lower values of $R_{A,n}$ and better overall agreement to the models, when compared to the fixed v_d method. The fixed v_d flux comparison for TM4 was also worse ($R_{A,n}$ was higher) than the TM4 concentration comparison, which was caused by the value of v_d used in the calculation being higher than the average deposition velocities used in TM4 or the variable v_d calculation.

Figures 8 – 13 show the spatial distribution of CalDep for each of the three study regions, together with the corresponding ModDep fields from ACCMIP and TM4. From these figures it is clear that the CalDep calculation method (fixed- and variable

Atmos. Chem. Phys. Discuss., doi:10.5194/acp-2016-1123, 2017
Manuscript under review for journal Atmos. Chem. Phys.
Published: 16 January 2017

v_d methods) influences both the magnitude and spatial distribution of N deposition estimates, and that this will, in turn, influence assessments of the impacts of that deposition on the marine environment.

3.4.1 Tropical Eastern Atlantic

For NO_3^-, this was the region with the best overall agreement between CalDep and the modelled fluxes ($R_{A,n}$ values of 0.6 – 1.1). However, as with the concentration comparison (Fig. 5), the spatial distributions of CalDep and ModDep were rather different. All of the models predicted a decreasing gradient in NO_y / NO_3^- deposition from northeast to southwest across the region, while the CalDep fluxes were greatest off the coast of North Africa in the latitude band 10° - 25°N (Fig. 8). The TM4 NO_3^- deposition field did indicate slightly higher fluxes in this area, but did not reproduce the magnitude of the CalDep fluxes there.

The NH_4^+ CalDep fields show rather uniform distributions in the TEAtl region (Fig. 9). Both the spatial distribution and magnitude of the observed fluxes appear to be rather well reproduced by the TM4 NH_4^+ simulation ($R_{A,n}$ = 0.9 – 1.1).

3.4.2 Northern Indian Ocean

In the NInd region, all of the models indicate a strong north – south gradient in NO_y / NO_3^- deposition (Fig. 10). While there is a north – south gradient in NO_3^- CalDep over the Arabian Sea, CalDep fluxes over the Bay of Bengal were as low as those in the south of the region. This discrepancy over the Bay of Bengal contributes to the general over-estimation by the models over the region as a whole ($R_{A,n}$ values of 1.2 – 2.6).

NH_4^+ CalDep fluxes were relatively high in the Bay of Bengal and to the southwest of southern India, but low in most of the Arabian Sea. The TM4 NH_4^+ simulation (Fig. 11f) indicated deposition further to the northwest of the Arabian Sea than the CalDep fluxes and slightly underestimated deposition to the Bay of Bengal, but gave good agreement for the region as a whole ($R_{A,n}$ values of 0.9 – 1.1).

3.4.3 Northwest Pacific margins

Although there were rather few grid cells with good data coverage in this region, for most cells the modelled NO_y / NO_3^- deposition was similar to NO_3^- CalDep (Fig. 7; $R_{A,n}$ = 1.5 – 2.2). The CalDep fluxes appear to show a strong northwest – southeast gradient in deposition, as indicated by the models (Fig. 12). However, the models appear to over-estimate the deposition of NO_3^- around the south and east of Korea and the south of Japan. The highest NO_3^- CalDep fluxes occurred closer to the coast of China than was simulated in the models.

The spatial distribution of NH_4^+ deposition (CalDep and ModDep) appears to be dominated by a similar northwest – southeast gradient to NO_3^- (Fig. 13). Agreement between CalDep for NH_4^+ and ModDep from TM4 was relatively good in this region, with slight under-estimation by the model ($R_{A,n}$ values of 0.6 – 0.8).

Atmos. Chem. Phys. Discuss., doi:10.5194/acp-2016-1123, 2017
Manuscript under review for journal Atmos. Chem. Phys.
Published: 16 January 2017

4 Discussion

The comparisons presented above highlight a number of cases where the spatial distribution or magnitude of observed concentrations or CalDep were not reproduced by the model products. In most cases, there is not sufficient information available to make a detailed analysis of these discrepancies. However, a discussion of potential sources of bias and divergence between observations and models is set out below.

4.1 Bias in observed concentrations and calculated deposition fluxes

Inertial segregation of larger particles at inlets of aerosol sampling systems, particularly at higher wind velocities, can result in relatively low passing/collection efficiencies and thus negative bias for super-micron aerosol constituents including NO_3^-. Cascade impactors are associated with significant internal losses (typically ranging from 25% to 40%) of large particles (e.g. Young et al., 2013; Marple et al., 1991). Because virtually all NO_3^- in marine air is associated with super-micron diameter particles, NO_3^- concentrations summed over all impactor size fractions correspond to lower limits for ambient concentrations and dry deposition fluxes estimated from those concentrations.

The pH of marine aerosol varies significantly as a function of size. In addition, based on their thermodynamic properties, the gas-aerosol phase partitioning of nitric acid (HNO_3) and NH_3 vary as a function of pH. HNO_3 partitions preferentially with the less acidic super-micron size fractions, while NH_3 partitions preferentially with the highly acidic sub-micron size fractions. When chemically distinct aerosol size fractions are sampled in bulk, the pH of the bulk mixture differs from that of the size fractions with which HNO_3 and NH_3 partition preferentially in air. This drives artefact phase changes of both HNO_3 and NH_3, resulting in negative measurement bias. Because of their relatively short atmospheric lifetimes, low surface-to-volume ratios, and corresponding slow rates of thermodynamic equilibrium, the upper-end of the marine aerosol size distribution is often under-saturated with respect to gaseous HNO_3. Following collection on filters, HNO_3 can continue to condense from the sample air stream into these particle deposits resulting in positive measurement bias. In addition, a number of aerosol collection media have been reported to be susceptible to uptake of gas-phase species such as HNO_3 and NH_3 (e.g. Keck and Wittmaack, 2005).

Thus, there are a variety of processes that can lead to positive and negative biases in measured aerosol NO_3^- and NH_4^+ concentrations, particularly in the marine environment. If such effects have influenced the database used here, biases are unlikely to be uniform across all the observations, since the observations come from a very wide variety of sources with many different sample collection protocols.

Dry deposition velocities are subject to high levels of uncertainty (up to a factor of 2 - 3 (Duce et al., 1991)), due to their strongly non-linear variation with parameters such as particle size, wind speed and deposition surface properties (Slinn and Slinn, 1980). Their use to estimate CalDep fluxes here therefore introduces substantial uncertainty into the CalDep – ModDep flux comparison.

Atmos. Chem. Phys. Discuss., doi:10.5194/acp-2016-1123, 2017
Manuscript under review for journal Atmos. Chem. Phys.
Published: 16 January 2017

4.2 Divergence between modelled and actual aerosol concentrations and deposition fluxes

In addition to the sampling-related biases discussed above, differences between observations and model calculations for a given grid cell can originate from several other inter-related processes. These include differences between the following modelled and actual processes: upwind emissions (including long-term trends in emissions) of NO_x and NH_3 and associated transport regimes; upwind chemical transformations and removal; phase partitioning of HNO_3 and NH_3 with size-resolved particles in near-surface marine air and the corresponding size distributions of particulate NO_3^- and NH_4^+. In the latter case, if simulated concentrations of total NO_3 (HNO_3 + NO_3^-) and NH_3 (NH_3 + NH_4^+) were in agreement with actual concentrations but gas-phase concentrations were over-estimated, particulate-phase concentration (and dry fluxes) would be under-estimated. In addition, even if the total concentrations of particulate NO_3^- and NH_4^+ were modelled correctly, incorrectly simulated or assumed size distributions would lead to incorrect dry deposition fluxes, because dry deposition velocities vary greatly as a function of particle size. Gas-aerosol phase partitioning is highly parameterized in most global models. For particulates with deposition velocity of the order of 1 cm s^{-1} (i.e. NO_3^-), the short vertical turnover time of the surface atmospheric layer can lead to strong surface concentration gradients. This can lead to biases in the comparison of vertically averaged (for instance over 50 m in TM4) modelled surface layer concentration (or deposition flux) with observations made at heights that vary depending on the ships used for sampling (typically 10-20 m).

As stated above, dry deposition velocities are highly uncertain. If modelled and observed aerosol concentrations were in agreement, differences between modelled dry deposition velocities for size-resolved particles and those used to calculate dry deposition fluxes from observed aerosol concentrations would lead to model – observation divergence. In addition, bias in estimated deposition velocities for gases also impacts lifetimes of modelled total NO_3 and NH_3, which would in turn influence the concentrations and dry fluxes of particulate N.

Differences between modelled and actual deposition modes for HNO_3/NO_3^- and NH_3/NH_4^+ can also influence model – observation comparison. For instance, over-estimation of modelled wet fluxes of total NO_3 and NH_3, would lead to under-estimation of their modelled dry fluxes. Wet deposition is also highly parameterized in most global models.

The extent to which the available observations represent the actual conditions of the areas studied will also influence the effectiveness of the model – observation comparison. Ideally, the observations should capture the spatial variability of aerosol concentrations across the area to be compared (particularly for regions with large gradients, such as those across coasts), and should also be representative of temporal variations (i.e. observations distributed throughout the year are required to capture the annual mean concentration for species / regions with high seasonality). The 16-year period over which the observational database was acquired may also influence the effectiveness of the comparison to the shorter timescales represented by the model products.

Atmos. Chem. Phys. Discuss., doi:10.5194/acp-2016-1123, 2017
Manuscript under review for journal Atmos. Chem. Phys.
Published: 16 January 2017

Atmospheric Chemistry and Physics Discussions

388 **4.3 Influence of seasonality**

389 Because there were few grid cells for which the observational data covered the majority of a calendar year, it was possible that
390 unrepresentative sampling of seasonal variations in aerosol concentrations might lead to apparent biases in the annual-based
391 observation – model comparisons reported in this paper.

392 The potential impact of seasonality was examined for the TEAtl, NInd and NWPac study regions, by comparing monthly mean
393 NO_3^- and NH_4^+ concentrations simulated by TM4 to observations in individual grid cells that contained relatively large
394 numbers of observations (Fig. 3). For most cells, the TM4 simulation of both N species was very similar to the available ship-
395 and island-based observations. However, in the Indian Ocean cells (C and D) there appeared to be relatively strong seasonality
396 that was not always well-reproduced by the model. For instance, TM4 appeared to under-estimate observed median NH_4^+
397 concentrations in cell C during the months of January to March by factors of 2 – 3 (Fig. 3i), and over-estimated observed
398 median NO_3- concentrations in cell D by factors of at least 4, with the seasonal changes indicated by the model not being
399 evident in the observations (Fig. 3d).

400 On the scale of the whole study regions, observed seasonality was reproduced best by TM4 in the TEAtl region (Fig. 14 a &
401 d). In the NInd region, TM4 predicted a strong seasonal cycle for NO_3^- (particularly in the Arabian Sea (Fig. S8)) which was
402 not entirely reflected in the observed concentrations (Fig. 14b). Observed NH_4^+ seasonality in the NInd appears to be more
403 pronounced than simulated in the model (Fig. 14e). Note that the uneven distribution of sample numbers through the year is a
404 potential source of bias in the monthly mean observed concentrations used to infer seasonal cycles here. Since the comparisons
405 of annual mean observed concentrations with those simulated by TM4 indicated differences over the Arabian Sea and Bay of
406 Bengal (Fig. 5 and 6), observed and TM4 monthly concentrations and monthly total numbers of observations for these two
407 regions (5°-25°N, 55°-75°E and 5°-25°N, 80°-90°E respectively) are shown in Fig. 15. This shows clear differences in the
408 temporal distribution of sample collection between the Arabian Sea and Bay of Bengal, with sampling over the latter dominated
409 by the period of outflow from the Indo-Gangetic Plain (Srinivas et al., 2014). There were also differences in the extent to which
410 the model predicted seasonal variations in NO_3^- and NH_4^+ concentrations (Fig. 15). For NO_3^-, TM4 simulated a strong seasonal
411 variation over the Arabian Sea (and the observed months cover the full range of predicted concentration change), but a much
412 weaker seasonality over the Bay of Bengal. The available observations suggest that the NO_3^- seasonal cycles are more
413 pronounced than predicted for the Arabian Sea and Bay of Bengal and that TM4 over-predicts mean NO_3^- concentrations in
414 the Bay of Bengal by factors of 2 – 25 in all months with observations. For NH_4^+, there was strong seasonality in the TM4
415 concentration over both areas, but almost all the observations from the Arabian Sea were from months when TM4 predicted
416 low concentrations, while the period of lowest concentrations predicted over the Bay of Bengal was almost entirely missing
417 from the observations. Thus, it seems very likely that seasonality contributed to divergence between the models and
418 observations over the NInd region for NH_4^+, but was less important for NO_3^- there. (Note that these analyses of seasonality at
419 the regional-scale allow investigation of the model – observation comparison, but cannot provide assurance that either the

Atmos. Chem. Phys. Discuss., doi:10.5194/acp-2016-1123, 2017
Manuscript under review for journal Atmos. Chem. Phys.
Published: 16 January 2017

ship-based observations, or the model, reproduce accurately the annual mean aerosol concentrations, especially in the NInd region, where there are no independent seasonal records available).

4.4 Role of mineral dust in modifying N deposition fluxes

It is not entirely coincidental that all three of the study regions examined in this paper are impacted strongly by transport and deposition of mineral dust. Interest in the impact of dust deposition on marine productivity (Jickells et al., 2005) has stimulated a great deal of research into aerosol chemistry at the outflows of the world's major deserts over the past few decades (e.g. Gao et al., 2007; Baker et al., 2013; Srinivas and Sarin, 2013; Srinivas et al., 2014; Powell et al., 2015). Much of the observational work on dust has generated data on aerosol N concentrations, augmenting the data available in these regions, but the presence of dust adds extra complexity to the comparison performed here. Uptake of nitric acid onto suspended mineral dust particles alters the size distribution and deposition velocity of aerosol nitrate, as well as changing the gas-phase composition of N (Hanisch and Crowley, 2001; Rubasinghege and Grassian, 2009). Atmospheric chemical-transport models for N must therefore also incorporate effective simulations of mineral dust. This is itself a considerable challenge, with atmospheric dust models generally only reproducing surface dust concentrations within a factor of 10 (Huneeus et al., 2011) and failing to reproduce key aspects of the dust cycle even in well-characterised regions (Prospero et al., 2010).

4.5 Challenges posed by uncertainty in dry deposition velocities

As noted above, dry deposition velocities are probably the largest sources of uncertainty in estimates of dry deposition fluxes of aerosol components. Thus the comparisons of observed and modelled aerosol concentrations presented in Fig. 4 – 6 are preferable to comparisons of dry deposition flux because they avoid the uncertainty associated with conversion of measured aerosol concentrations into CalDep. However, modelled aerosol concentrations at a given location are dependent on the parameterisation of dry deposition velocity (together with a number of other factors of varying degrees of uncertainty) applied by the model all along the simulated aerosol transport pathway. Uncertainty in modelled v_d therefore also impacts the effectiveness of the concentration comparison, although gross errors in v_d in models are unlikely to result in good agreement between observed and simulated aerosol concentrations.

5 Conclusions

A unique dataset of particulate NO_3^- and NH_4^+ concentrations in the marine atmosphere was compiled, based on 2890 samples from oceanographic cruises between 1995 and 2012. The data were mapped to 5° x 5° grid cells and annual average concentrations were calculated for each cell. Dry deposition fluxes for each cell were calculated from these average concentrations.

Atmos. Chem. Phys. Discuss., doi:10.5194/acp-2016-1123, 2017
Manuscript under review for journal Atmos. Chem. Phys.
Published: 16 January 2017

Atmospheric Chemistry and Physics Discussions

Gridded concentrations and calculated dry deposition fluxes were compared with two different model products: The ACCMIP multi-model mean products of NO_y and NH_x dry deposition, and the TM4 model of NO_y and NH_x deposition fluxes and NO_3^- and NH_4^+ aerosol concentrations and deposition fluxes.

In general, the model-observation comparison exercise for the oceans attempted here is more difficult than a comparable exercise over land, due to the much more limited numbers of observations available over the oceans. Field campaigns that target key areas of uncertainty (such as in regions with strong seasonal cycles; intense gradients in N concentrations / deposition; and with contrasting mineral dust regimes) will be required to address these limitations.

Comparisons of deposition fluxes of NO_y and NH_x from the ACCMIP MMM product and from TM4 with observational-derived fluxes (CalDep) show similar performances for both products, with significant over-estimation of the lower levels of observed NH_4^+ deposition fluxes. ModDep of NO_3^- and NH_4^+ from TM4 show much better agreement with CalDep than did NO_y and NH_x, which is consistent with significant contributions of gaseous deposition to NO_y and NH_x deposition fluxes.

Given the uncertainties involved in the observations and modelling, it may be that the large scatter in the observation – model comparisons (Figs. 4, 7 and S5) are the best that can be achieved currently in this type of comparison. Uncertainties in dry deposition velocities remain a serious obstacle to improving observation- and modelling-based estimates of the atmospheric flux of material into the ocean. For example, if a given observation of aerosol NO_3^- concentration leads to a value of CalDep of 0.1 mg N m^{-2} d^{-1}, that value represents, at best, a flux in the range of 0.05 – 0.2 mg N m^{-2} d^{-1}. When considering modelled dry N deposition, the uncertainty in v_d (when compounded with the other sources of uncertainty in the modelling) probably implies that fluxes can be estimated to within no better than an order of magnitude. The uncertainty in modelled dry deposition, in turn, leads to uncertainty in modelled wet deposition estimates. This limitation has consequences for the usefulness of models in predicting the impacts of N deposition fluxes on the ocean, both in the present and into the future (Duce et al., 2008; Jickells et al., 2016). Understanding of the dry deposition of particulate matter to the ocean surface has not advanced for several decades (Slinn and Slinn, 1980) and concerted community action is required if further progress is to be made.

The approach to assessing the performance of N deposition models used here has some obvious limitations. It does, however, offer additional benefits to those provided by comparison to land-based wet deposition networks, in terms of both increasing the geographical distribution of comparative data and in extending the comparison to dry deposition. In the case of N deposition to the ocean, it is very unlikely that a coherent geographically-dispersed database of wet deposition observations will ever be available for this purpose. It is recommended strongly that future model validation and intercomparison exercises should incorporate comparisons to directly-measured aerosol concentrations, rather than to calculated dry deposition fluxes, which are currently subject to large uncertainties. Reporting of surface-level aerosol concentrations should therefore be considered a core requirement for future model intercomparison exercises.

Atmos. Chem. Phys. Discuss., doi:10.5194/acp-2016-1123, 2017
Manuscript under review for journal Atmos. Chem. Phys.
Published: 16 January 2017

Atmospheric Chemistry and Physics Discussions

Author Contribution

Study was designed by participants in a GESAMP WG38 workshop in 2013 (ARB, MK, KEA, GSO, FD, MU, MMS, RAD, AS, LZ, JMP), led by ARB. ARB, MU, MMS and SCH contributed data and MK, ND, SM, FD and JFL contributed model products. The workshop participants and ND established the observation – model comparison protocol. SSR helped to establish the COST735 Aerosol and Rainfall Chemistry Database, from which much of the data used was obtained. ARB and MK drafted the manuscript with contributions from all authors.

Competing Interests

The authors declare that they have no conflict of interest.

Acknowledgments

This paper resulted from the deliberations of GESAMP Working Group 38, the Atmospheric Input of Chemicals to the Ocean. We thank the ICSU Scientific Committee on Oceanic Research (SCOR), the US National Science Foundation (NSF), the Global Atmosphere Watch (GAW) and the World Weather Research Programme (WWRP) of the World Meteorological Organization (WMO), the International Maritime Organization (IMO), the University of Crete and the University of East Anglia for support of this work. ARB's contribution to this work was supported by grant NE/H00548X/1 from the UK Natural Environment Research Council. Thanks to several colleagues, named in Table S1, who contributed data to this work.

Figure Captions

Figure 1. Spatial distribution of the a) aerosol samples and the distributions of these samples by b) month and c) year for the entire database divided according to the main ocean basins.

Figure 2. Aerosol sample collection start locations in the a) TEAtl, b) NInd and c) NWPac regions. Samples with NO_3^- observations are indicated with blue crosses and those with NH_4^+ observations by red circles. Data for grid cells A – F are shown in detail in Fig. 3.

Figure 3. Box and whisker plots, showing the distribution of aerosol NO_3^- (left) and NH_4^+ (right) concentrations (nmol m^{-3}) in selected grid cells from the TEAtl, NInd and NWPac regions. Upper and lower limits of boxes represent the interquartile range of data in each category, with the median shown as bars in each box. Whiskers represent the range of the data, except where extremes (values greater than 1.5 times the interquartile range above the upper quartile) were present (crosses). Where only 1 data point was available for a given month, this is shown as a solid bar. Summaries of longer-term aerosol sampling records for the Cape Verde Islands (a) & g)) and Pengchiayu Island (e) & k)) are also shown. In those panels, red dashed and dotted lines represent the mean, minimum and maximum concentrations of all the island data, while open circles represent the monthly mean concentrations for all of the observations in each island record. Monthly mean concentrations from the TM4 model are shown for each cell as blue triangles. Locations of the cells A – F are shown in Fig. 2.

Figure 4. Scatter plots comparing mean 5° x 5° grid cell aerosol concentrations of a) NO_3^- and b) NH_4^+ from the observational database with corresponding concentrations from the TM4 model. Data are plotted for each grid cell

Atmos. Chem. Phys. Discuss., doi:10.5194/acp-2016-1123, 2017
Manuscript under review for journal Atmos. Chem. Phys.
Published: 16 January 2017

Atmospheric Chemistry and Physics Discussions

that contains observational data (grey), with cells from the TEAtl, NInd and NWPac regions coloured blue, orange and red respectively. Marker size is proportional to numbers of observations in each cell, with the smallest marker representing 5 or fewer observations and the largest more than 15 observations. Solid lines indicate 1:1 observation – model relationship, dashed lines correspond to observation – model ratios of 10:1 and 1:10 in each panel. The weighted model : observation ratio ($R_{A,n}$) and the normalised mean bias are given for each region.

Figure 5. Mean observed aerosol NO_3^- concentrations (left column) and their concentrations simulated by TM4 (right column), for the eastern tropical Atlantic (a & d), northern Indian (b & e) and northwest Pacific (c & f) study regions.

Figure 6. Mean observed aerosol NH_4^+ concentrations (left column) and their concentrations simulated by TM4 (right column), for the eastern tropical Atlantic (a & d), northern Indian (b & e) and northwest Pacific (c & f) study regions.

Figure 7. Scatter plots comparing dry deposition fluxes (mg N m^{-2} d^{-1}) of a) – c) NO_3^- and d) – f) NH_4^+ derived from the observational database with corresponding fluxes from model output. Panels represent comparisons to a) NO_y from ACCMIP, b) NO_y from TM4, c) NO_3^- from TM4, d) NH_x from ACCMIP, e) NH_x from TM4 and f) NH_4^+ from TM4. CalDep calculated by the variable v_d method. Explanations of marker sizes and colours are given in the legend for Fig. 4.

Figure 8. Dry deposition fluxes (mg N m^{-2} d^{-1}) for NO_3^- / NO_y for the TEAtl region. Panels show a) numbers of samples per grid cell (upper left, blue) and number of calendar months represented by observations (lower right, red), NO_3^- CalDep calculated using the b) fixed v_d and c) variable v_d methods, d) NO_y ModDep from ACCMIP, e) NO_y ModDep from TM4 and f) NO_3^- ModDep from TM4.

Figure 9. Dry deposition fluxes (mg N m^{-2} d^{-1}) for NH_4^+ / NH_x for the TEAtl region. Panels show a) numbers of samples per grid cell (upper left, blue) and number of calendar months represented by observations (lower right, red), NH_4^+ CalDep calculated using the b) fixed v_d and c) variable v_d methods, d) NH_x ModDep from ACCMIP, e) NH_x ModDep from TM4 and f) NH_4^+ ModDep from TM4.

Figure 10. Dry deposition fluxes (mg N m^{-2} d^{-1}) for NO_3^- / NO_y for the NInd region. Panels are as described in Fig. 8.

Figure 11. Dry deposition fluxes (mg N m^{-2} d^{-1}) for NH_4^+ / NH_x for the NInd region. Panels are as described in Fig. 9.

Figure 12. Dry deposition fluxes (mg N m^{-2} d^{-1}) for NO_3^- / NO_y for the NWPac region. Panels are as described in Fig. 8.

Figure 13. Dry deposition fluxes (mg N m^{-2} d^{-1}) for NH_4^+ / NH_x for the NWPac region. Panels are as described in Fig. 9.

Figure 14. Monthly mean observed aerosol concentrations (red circles), simulated concentrations from TM4 (blue triangles) and total number of observations in each month (bars) for NO_3^- (left) and NH_4^+ (right) for the TEAtl (a & d), NInd (b & e) and NWPac (c & f) regions.

Figure 15. Monthly mean observed aerosol concentrations (red circles), simulated concentrations from TM4 (blue triangles)) and total number of observations (n) in each month (bars) for NO_3^- (left) and NH_4^+ (right) for the Arabian Sea (a & c) and Bay of Bengal (b & d).

Atmos. Chem. Phys. Discuss., doi:10.5194/acp-2016-1123, 2017
Manuscript under review for journal Atmos. Chem. Phys.
Published: 16 January 2017

Atmospheric Chemistry and Physics Discussions

Tables

Table 1. Description of the observational databases for NO_3^- and NH_4^+ for the whole ocean, TEAtl, NInd and NWPac regions. Number of observations (n^{obs}), number (and percentage) of oceanic grid cells containing observations (n^{cells}), percentage of ocean cells containing ≥ 10 observations (O10), and percentage of ocean grid cells with observations in ≥ 4 months (M4) are given for each region.

	NO_3^-	NH_4^+
Whole Ocean		
n^{obs}	2800	2424
n^{cells}	550 (28%)	478 (24%)
O10 (%)[a]	12	12
M4 (%)[a]	13	10
TEAtl		
n^{obs}	491	375
n^{cells}	36 (97%)	36 (97%)
O10 (%)[a]	56	44
M4 (%)[a]	72	53
NInd		
n^{obs}	507	473
n^{cells}	42 (91%)	40 (87%)
O10 (%)[a]	48	41
M4 (%)[a]	43	28
NWPac		
n^{obs}	263	252
n^{cells}	22 (79%)	20 (71%)
O10 (%)[a]	32	25
M4 (%)[a]	41	40

a – calculated for grid cells containing observations only

Atmos. Chem. Phys. Discuss., doi:10.5194/acp-2016-1123, 2017
Manuscript under review for journal Atmos. Chem. Phys.
Published: 16 January 2017

Atmospheric Chemistry and Physics Discussions

Table 2. Summary of areal average CalDep and ModDep fluxes (F, mg N m^{-2} d^{-1}) of NO_3^-/NO_y and NH_4^+/NH_x for grid cells containing observations for the whole ocean and the TEAtl, NInd and NWPac regions.

	CalDep				ModDep			
	Fixed v_d		Variable v_d					
	NO_3^-	NH_4^+	NO_3^-	NH_4^+	NO_3^-	NO_y	NH_4^+	NH_x
Whole Ocean								
F	0.098	0.024	0.079	0.031				
F ACCMIP						0.098		0.060
F TM4					0.101	0.116	0.022	0.074
TEAtl								
F	0.182	0.021	0.139	0.026				
F ACCMIP						0.107		0.046
F TM4					0.133	0.142	0.019	0.042
NInd								
F	0.149	0.060	0.099	0.067				
F ACCMIP						0.116		0.098
F TM4					0.132	0.151	0.040	0.112
NWPac								
F	0.280	0.080	0.233	0.108				
F ACCMIP						0.335		0.144
F TM4					0.265	0.311	0.064	0.116

Atmos. Chem. Phys. Discuss., doi:10.5194/acp-2016-1123, 2017
Manuscript under review for journal Atmos. Chem. Phys.
Published: 16 January 2017

Atmospheric Chemistry and Physics Discussions

References

Baker, A. R., Lesworth, T., Adams, C., Jickells, T. D., and Ganzeveld, L.: Estimation of atmospheric nutrient inputs to the Atlantic Ocean from 50°N to 50°S based on large-scale field sampling: Fixed nitrogen and dry deposition of phosphorus, Global Biogeochemical Cycles, 24, GB3006, 10.1029/2009GB003634, 2010.

Baker, A. R., Adams, C., Bell, T. G., Jickells, T. D., and Ganzeveld, L.: Estimation of atmospheric nutrient inputs to the Atlantic Ocean from 50°N to 50°S based on large-scale field sampling: Iron and other dust-associated elements, Global Biogeochemical Cycles, 27, 755-767, 10.1002/gbc.20062, 2013.

Baker, A. R., Thomas, M., Bange, H. W., and Plasencia Sánchez, E.: Soluble trace metals in aerosols over the tropical south-east Pacific offshore of Peru, Biogeosciences, 13, 817-825, 10.5194/bg-13-817-2016, 2016.

Bouwman, A. F., Lee, D. S., Asman, W. A. H., Dentener, F. J., VanderHoek, K. W., and Olivier, J. G. J.: A global high-resolution emission inventory for ammonia, Global Biogeochemical Cycles, 11, 561-587, 1997.

Buck, C. S., Landing, W. M., and Resing, J.: Pacific Ocean aerosols: Deposition and solubility of iron, aluminum, and other trace elements, Marine Chemistry, 157, 117-130, 10.1016/j.marchem.2013.09.005, 2013.

Chien, C.-T., Mackey, K. R. M., Dutkiewicz, S., Mahowald, N. M., Prospero, J. M., and Paytan, A.: Effects of African dust deposition on phytoplankton in the western tropical Atlantic Ocean off Barbados, Global Biogeochemical Cycles, 30, 716-734, 10.1002/2015GB005334, 2016.

Chung, C. C., Chang, J., Gong, G. C., Hsu, S. C., Chiang, K. P., and Liao, C. W.: Effects of Asian Dust Storms on Synechococcus populations in the subtropical Kuroshio Current, Marine Biotechnology, 13, 751-763, 10.1007/s10126-010-9336-5, 2011.

Dentener, F., Drevet, J., Lamarque, J. F., Bey, I., Eickhout, B., Fiore, A. M., Hauglustaine, D., Horowitz, L. W., Krol, M., Kulshrestha, U. C., Lawrence, M., Galy-Lacaux, C., Rast, S., Shindell, D., Stevenson, D., van Noije, T., Atherton, C., Bell, N., Bergman, Butler, T., Cofala, J., Collins, B., Doherty, R., Ellingsen, K., Galloway, J., Gauss, M., Montanaro, V., Muller, J. F., Pitari, G., Rodriguez, J., Sanderson, M., Solmon, F., Strahan, S., Schultz, M., Sudo, K., Szopa, S., and Wild, O.: Nitrogen and sulfur deposition on regional and global scales: A multimodel evaluation, Global Biogeochemical Cycles, 20, GB4003, 10.1029/2005GB002672, 2006.

Duce, R. A., Liss, P. S., Merrill, J. T., Atlas, E. L., Buat-Menard, P., Hicks, B. B., Miller, J. M., Prospero, J. M., Arimoto, R., Church, T. M., Ellis, W., Galloway, J. N., Hansen, L., Jickells, T. D., Knap, A. H., Reinhardt, K. H., Schneider, B., Soudine, A., Tokos, J. J., Tsunogai, S., Wollast, R., and Zhou, M.: The atmospheric input of trace species to the world ocean, Global Biogeochemical Cycles, 5, 193-259, 10.1029/91GB01778, 1991.

Duce, R. A., La Roche, J., Altieri, K., Arrigo, K. R., Baker, A. R., Capone, D. G., Cornell, S., Dentener, F., Galloway, J., Ganeshram, R. S., Geider, R. J., Jickells, T., Kuypers, M. M., Langlois, R., Liss, P. S., Liu, S. M., Middleburg, J. J., Moore, C. M., Nickovic, S., Oschlies, A., Pedersen, T., Prospero, J., Schlitzer, R., Seitzinger, S., Sorensen, L. L., Uematsu, M., Ulloa, O., Voss, M., Ward, B., and Zamora, L.: Impacts of atmospheric anthropogenic nitrogen on the open ocean, Science, 320, 893-897, 2008.

Fomba, K. W., Müller, K., van Pinxteren, D., Poulain, L., van Pinxteren, M., and Herrmann, H.: Long-term chemical characterization of tropical and marine aerosols at the Cape Verde Atmospheric Observatory (CVAO) from 2007 to 2011, Atmospheric Chemistry and Physics, 14, 8883-8904, 10.5194/acp-14-8883-2014, 2014.

Fountoukis, C., and Nenes, A.: ISORROPIA II: a computationally efficient thermodynamic equilibrium model for K^+-Ca^{2+}-Mg^{2+}-NH_4^+-Na^+-SO_4^{2-}-NO_3^--Cl^--H_2O aerosols, Atmospheric Chemistry and Physics, 7, 4639-4659, 2007.

Galloway, J. N., Dentener, F. J., Capone, D. G., Boyer, E. W., Howarth, R. W., Seitzinger, S. P., Asner, G. P., Cleveland, C. C., Green, P. A., Holland, E. A., Karl, D. M., Michaels, A. F., Porter, J. H., Townsend, A. R., and Vorosmarty, C. J.: Nitrogen cycles: past, present, and future, Biogeochemistry, 70, 153-226, 2004.

Galloway, J. N., Townsend, A. R., Erisman, J. W., Bekunda, M., Cai, Z., Freney, J. R., Martinelli, L. A., Seitzinger, S. P., and Sutton, M. A.: Transformations of the nitrogen cycle: Recent trends, questions, and potential solutions, Science, 320, 889-892, 2008.

Ganzeveld, L., Lelieveld, J., and Roelofs, G.-J.: A dry deposition parameterization of sulfur oxides in a chemistry and general circulation, Journal of Geophysical Research-Atmospheres, 103, 5679-5694, 1998.

Gao, Y., Anderson, J. R., and Hua, X.: Dust characteristics over the North Pacific observed through shipboard measurements during the ACE-Asia experiment, Atmospheric Environment, 41, 7907-7922, 2007.

Hanisch, F., and Crowley, J. N.: Heterogeneous reactivity of gaseous nitric acid on Al_2O_3, $CaCO_3$, and atmospheric dust samples: A Knudsen cell study, Journal of Physical Chemistry A, 105, 3096-3106, 2001.

Hsu, S. C., Lee, C. S. L., Huh, C. A., Shaheen, R., Lin, F. J., Liu, S. C., Liang, M. C., and Tao, J.: Ammonium deficiency caused by heterogeneous reactions during a super Asian dust episode, J. Geophys. Res., 119, 6803-6817, 10.1002/2013JD021096, 2014.

Huneeus, N., Schulz, M., Balkanski, Y., Griesfeller, J., Prospero, J., Kinne, S., Bauer, S., Boucher, O., Chin, M., Dentener, F., Diehl, T., Easter, R., Fillmore, D., Ghan, S., Ginoux, P., Grini, A., Horowitz, L., Koch, D., Krol, M. C., Landing, W., Liu, X., Mahowald, N., Miller, R., Morcrette, J. J., Myhre, G., Penner, J., Perlwitz, J., Stier, P., Takemura, T., and Zender, C. S.: Global dust model intercomparison in AeroCom phase I, Atmospheric Chemistry and Physics, 11, 7781-7816, 10.5194/acp-11-7781-2011, 2011.

Jickells, T. D., An, Z. S., Anderson, K. K., Baker, A. R., Bergametti, G., Brooks, N., Cao, J. J., Boyd, P. W., Duce, R. A., Hunter, K. A., Kawahata, H., Kubilay, N., La Roche, J., Liss, P. S., Mahowald, N., Prospero, J. M., Ridgwell, A. J., Tegen, I., and Torres, R.: Global Iron Connections between desert dust, ocean biogeochemistry and climate, Science, 308, 67-71, 2005.

Jickells, T. D., Buitenhuis, E. T., Altieri, K., Baker, A. R., Capone, D., Duce, R. A., Dentener, F., Fennel, K., Kanakidou, M., LaRoche, J., Lee, K., Liss, P. S., Middelburg, J. J., Moore, J. K., Okin, G., Oschlies, A., Sarin, M., Seitzinger, S., Sharples, J., Suntharalingam, P., Uematsu, M., and Zamora, L. M.: A re-evaluation of the magnitude and impacts of anthropogenic atmospheric nitrogen inputs on the ocean, Global Biogeochemical Cycles, submitted, 2016.

Kanakidou, M., Duce, R., Prospero, J. M., Baker, A. R., Benitez-Nelson, C., Dentener, F. J., Hunter, K. A., Liss, P. S., Mahowald, N., Okin, G. S., Sarin, M., Tsigaridis, K., Uematsu, M., Zamora, L. M., and Zhu, T.: Atmospheric fluxes of organic N and P to the global ocean, Global Biogeochemical Cycles, 26, GB3026, 10.1029/2011GB004277, 2012.

Kanakidou, M., Myriokefalitakis, S., Daskalakis, N., Fanourgakis, G., Nenes, A., Baker, A. R., Tsigaridis, K., and Mihalopoulos, N.: Past, present and future atmospheric nitrogen deposition, Journal of Atmospheric Sciences, 73, 2039-2047, 10.1175/JAS-D-15-0278.1, 2016.

Karydis, V. A., Tsimpidi, A. P., Pozzer, A., Astitha, M., and Lelieveld, J.: Effects of mineral dust on global atmospheric nitrate concentrations, Atmospheric Chemistry and Physics, 16, 1491-1509, 10.5194/acp-16-1491-2016, 2016.

Keck, L., and Wittmaack, K.: Laboratory studies on the retention of nitric acid, hydrochloric acid and ammonia on aerosol filters, Atmospheric Environment, 39, 2157-2162, 10.1016/j.atmosenv.2004.12.021, 2005.

Keene, W. C., Galloway, J. N., Likens, G. E., Deviney, F. A., Mikkelsen, K. N., Moody, J. L., and Maben, J. R.: Atmospheric wet deposition in remote regions: Benchmarks for environmental change, Journal of the Atmospheric Sciences, 72, 2947-2978, 10.1175/JAS-D-14-0378.1, 2015.

Kim, T. W., Lee, K., Najjar, R. G., Jeong, H. D., and Jeong, H. J.: Increasing N Abundance in the Northwestern Pacific Ocean Due to Atmospheric Nitrogen Deposition, Science, 334, 505-509, 10.1126/science.1206583, 2011.

Lamarque, J. F., Dentener, F., McConnell, J., Ro, C. U., Shaw, M., Vet, R., Bergmann, D., Cameron-Smith, P., Dalsoren, S., Doherty, R., Faluvegi, G., Ghan, S. J., Josse, B., Lee, Y. H., MacKenzie, I. A., Plummer, D., Shindell, D. T., Skeie, R. B., Stevenson, D. S., Strode, S., Zeng, G., Curran, M., Dahl-Jensen, D., Das, S., Fritzsche, D., and Nolan, M.: Multi-model mean nitrogen and sulfur deposition from the Atmospheric Chemistry and Climate Model Intercomparison Project (ACCMIP): evaluation of historical and projected future changes, Atmospheric Chemistry and Physics, 13, 7997-8018, 10.5194/acp-13-7997-2013, 2013a.

Lamarque, J. F., Shindell, D. T., Josse, B., Young, P. J., Cionni, I., Eyring, V., Bergmann, D., Cameron-Smith, P., Collins, W. J., Doherty, R., Dalsoren, S., Faluvegi, G., Folberth, G., Ghan, S. J., Horowitz, L. W., Lee, Y. H., MacKenzie, I. A., Nagashima, T., Naik, V., Plummer, D., Righi, M., Rumbold, S. T., Schulz, M., Skeie, R. B., Stevenson, D. S., Strode, S., Sudo, K., Szopa, S., Voulgarakis, A., and Zeng, G.: The Atmospheric Chemistry and Climate Model Intercomparison Project (ACCMIP): overview and description of models, simulations and climate diagnostics, Geosci. Model Dev., 6, 179-206, 10.5194/gmd-6-179-2013, 2013b.

Landolfi, A., Dietze, H., Koeve, W., and Oschlies, A.: Overlooked runaway feedback in the marine nitrogen cycle: the vicious cycle, Biogeosciences, 10, 1351-1363, 10.5194/bg-10-1351-2013, 2013.

Markaki, Z., Oikonomou, K., Kocak, M., Kouvarakis, G., Chaniotaki, A., Kubilay, N., and Mihalopoulos, N.: Atmospheric deposition of inorganic phosphorus in the Levantine Basin, eastern Mediterranean: Spatial and temporal variability and its role in seawater productivity, Limnology and Oceanography, 48, 1557-1568, 2003.

Marple, V. A., Rubow, K. L., and Behm, S. M.: A microorifice uniform deposit impactor (MOUDI) - description, calibration, and use, Aerosol Science and Technology, 14, 434-446, 10.1080/02786829108959504, 1991.

Mourino-Carballido, B., Pahlow, M., and Oschlies, A.: High sensitivity of ultra-oligotrophic marine ecosystems to atmospheric nitrogen deposition, Geophysical Research Letters, 39, L05601, 10.1029/2011gl050606, 2012.

Myriokefalitakis, S., Daskalakis, N., Mihalopoulos, N., Baker, A. R., Nenes, A., and Kanakidou, M.: Changes in dissolved iron deposition to the oceans driven by human activity: a 3-D global modelling study, Biogeosciences, 12, 3973-3992, 10.5194/bg-12-3973-2015, 2015.

Powell, C. F., Baker, A. R., Jickells, T. D., Bange, H. W., Chance, R., and Yodle, C.: Estimation of the atmospheric flux of nutrients and trace metals to the eastern tropical North Atlantic Ocean, Journal of the Atmospheric Sciences of the American Meteorological Society, 72, 4029-4045, 10.1175/JAS-D-15-0011.1, 2015.

Prospero, J. M., Landing, W. M., and Schulz, M.: African dust deposition to Florida: Temporal and spatial variability and comparisons to models, J. Geophys. Res., 115, D13304, 10.1029/2009JD012773, 2010.

Rubasinghege, G., and Grassian, V. H.: Photochemistry of adsorbed nitrate on aluminum oxide particle surfaces, Journal of Physical Chemistry A, 113, 7818-7825, 2009.

Shi, J. H., Gao, H. W., Zhang, J., Tan, S. C., Ren, J. L., Liu, C. G., Liu, Y., and Yao, X. H.: Examination of causative link between a spring bloom and dry/wet deposition of Asian dust in the Yellow Sea, China, Journal of Geophysical Research-Atmospheres, 117, D17304, 10.1029/2012jd017983, 2012.

Singh, A., Gandhi, N., and Ramesh, R.: Contribution of atmospheric nitrogen deposition to new production in the nitrogen limited photic zone of the northern Indian Ocean, Journal of Geophysical Research-Oceans, 117, C06004, 10.1029/2011jc007737, 2012.

Slinn, S. A., and Slinn, W. G. N.: Predictions for particle deposition on natural waters, Atmospheric Environment, 14, 1013-1016, 1980.

Somes, C. J., Landolfi, A., Koeve, W., and Oschlies, A.: Limited impact of atmospheric nitrogen deposition on marine productivity due to biogeochemical feedbacks in a global ocean model, Geophysical Research Letters, 43, 4500-4509, 10.1002/2016gl068335, 2016.

Srinivas, B., and Sarin, M. M.: Atmospheric deposition of N, P and Fe to the Northern Indian Ocean: Implications to C- and N-fixation, Science of the Total Environment, 456-457, 104-114, 2013.

Srinivas, B., Sarin, M. M., and Rengarajan, R.: Atmospheric transport of mineral dust from the Indo-Gangetic Plain: Temporal variability, acid processing, and iron solubility, Geochemistry Geophysics Geosystems, 15, 3226-3243, 10.1002/2014gc005395, 2014.

Suntharalingam, P., Buitenhuis, E., Le Quere, C., Dentener, F., Nevison, C., Butler, J. H., Bange, H. W., and Forster, G.: Quantifying the impact of anthropogenic nitrogen deposition on oceanic nitrous oxide, Geophysical Research Letters, 39, L07605, 10.1029/2011gl050778, 2012.

Vet, R., Artz, R. S., Carou, S., Shaw, M., Ro, C.-U., Aas, W., Baker, A., Bowersox, V. C., Dentener, F., Galy-Lacaux, C., Hou, A., Pienaar, J. J., Gillett, R., Forti, M. C., Gromov, S., Hara, H., Khodzher, T., Mahowald, N. M., Nickovic, S., Rao, P. S. P., and Reid, N. W.: A global assessment of precipitation chemistry and deposition of sulfur, nitrogen, sea salt, base cations, organic acids, acidity and pH, and phosphorus, Atmospheric Environment, 93, 3-100, 10.1016/j.atmosenv.2013.10.060, 2014.

Young, A. H., Keene, W. C., Pszenny, A. A. P., Sander, R., Thornton, J. A., Riedel, T. P., and Maben, J. R.: Phase partitioning of soluble trace gases with size-resolved aerosols in near-surface continental air over northern Colorado, USA, during winter, J. Geophys. Res., 118, 9414-9427, 10.1002/jgrd.50655, 2013.

Zamora, L. M., Landolfi, A., Oschlies, A., Hansell, D. A., Dietze, H., and Dentener, F.: Atmospheric deposition of nutrients and excess N formation in the North Atlantic, Biogeosciences, 7, 777-793, 2010.

Atmos. Chem. Phys. Discuss., doi:10.5194/acp-2016-1123, 2017
Manuscript under review for journal Atmos. Chem. Phys.
Published: 16 January 2017

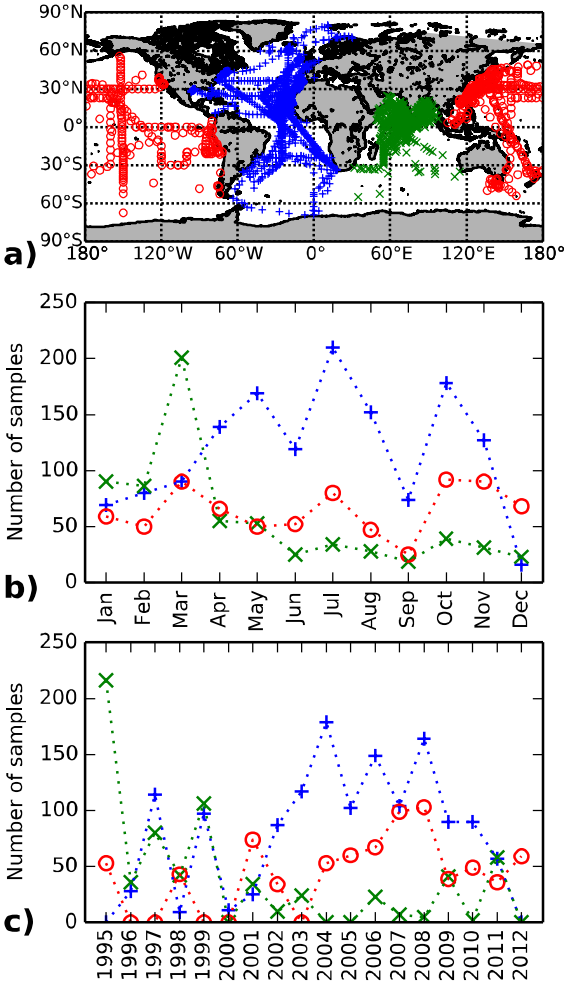

Fig. 1

Atmos. Chem. Phys. Discuss., doi:10.5194/acp-2016-1123, 2017
Manuscript under review for journal Atmos. Chem. Phys.
Published: 16 January 2017

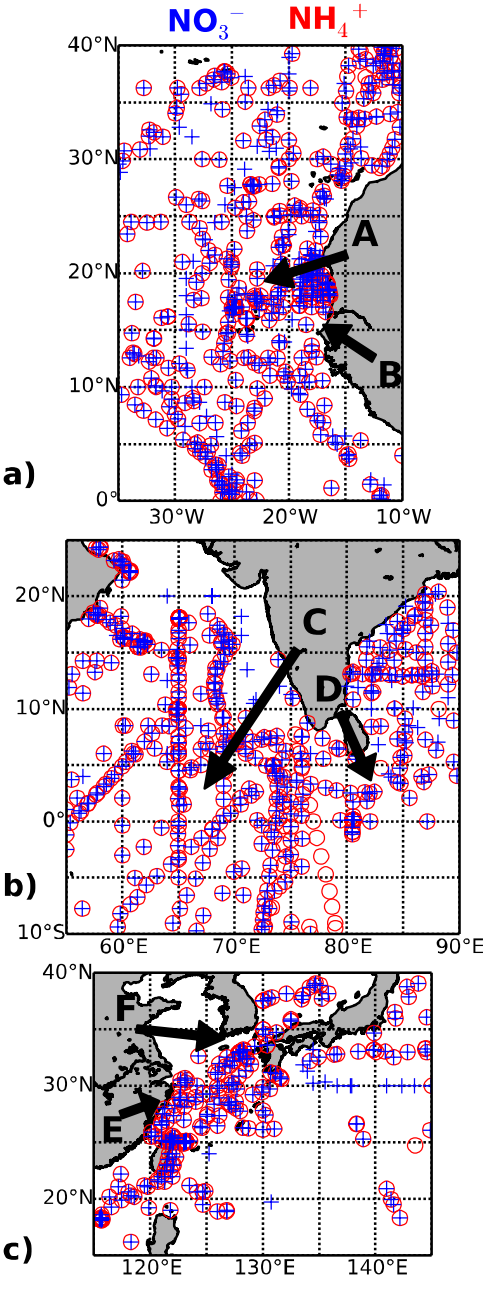

Fig. 2

Atmos. Chem. Phys. Discuss., doi:10.5194/acp-2016-1123, 2017
Manuscript under review for journal Atmos. Chem. Phys.
Published: 16 January 2017

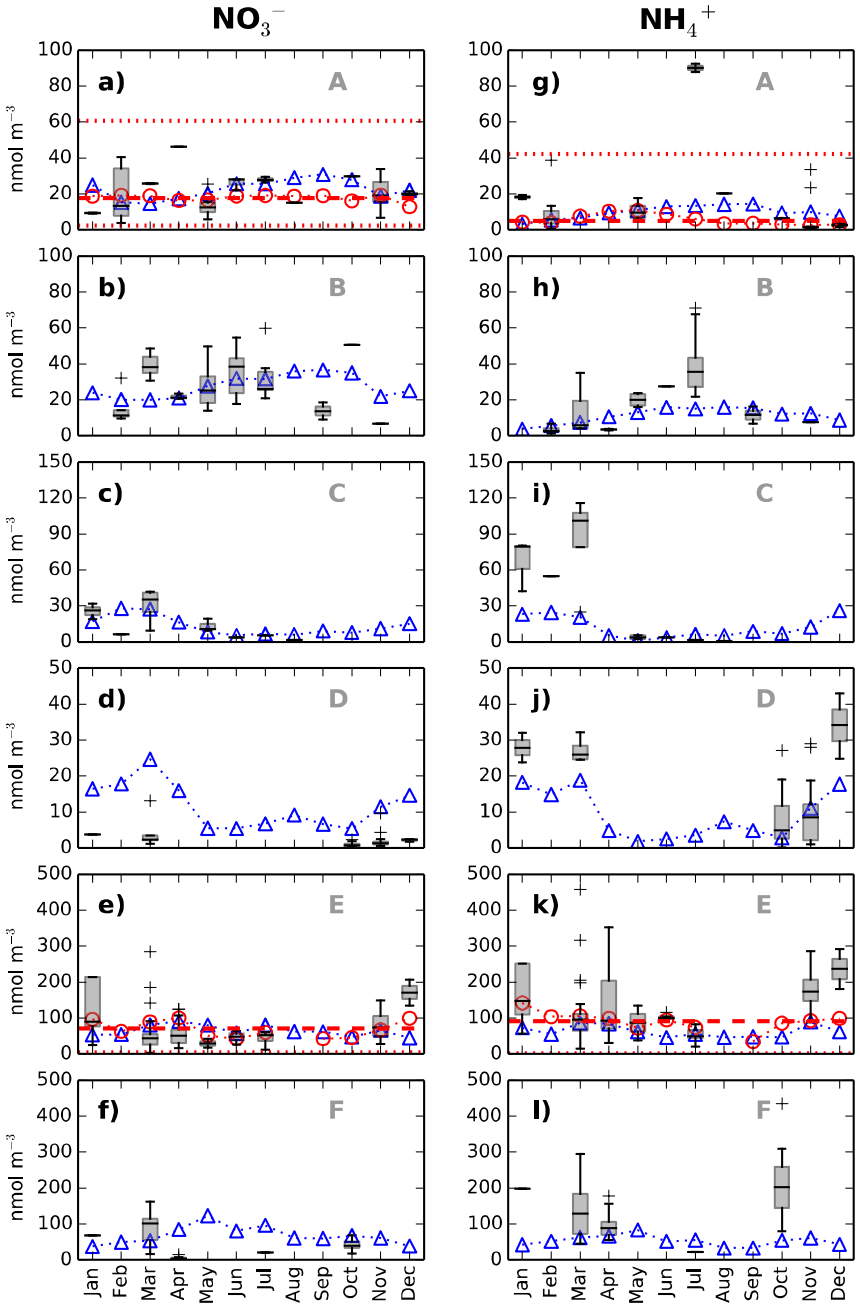

Fig. 3

Atmos. Chem. Phys. Discuss., doi:10.5194/acp-2016-1123, 2017
Manuscript under review for journal Atmos. Chem. Phys.
Published: 16 January 2017

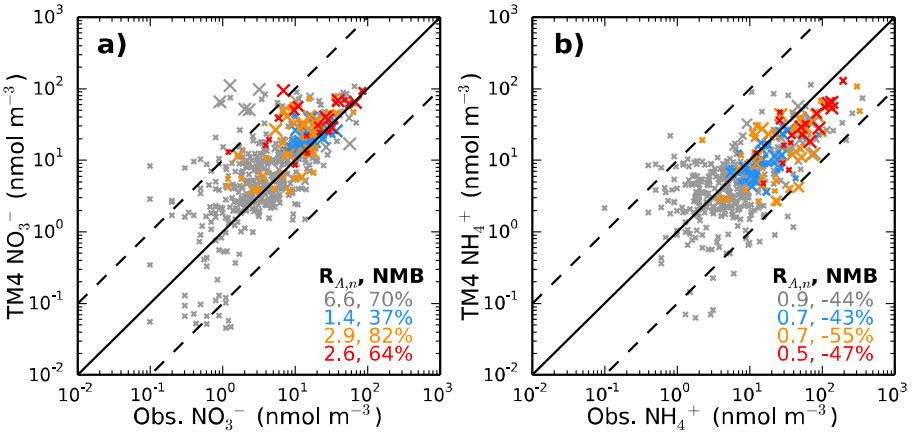

Fig. 4

Atmos. Chem. Phys. Discuss., doi:10.5194/acp-2016-1123, 2017
Manuscript under review for journal Atmos. Chem. Phys.
Published: 16 January 2017

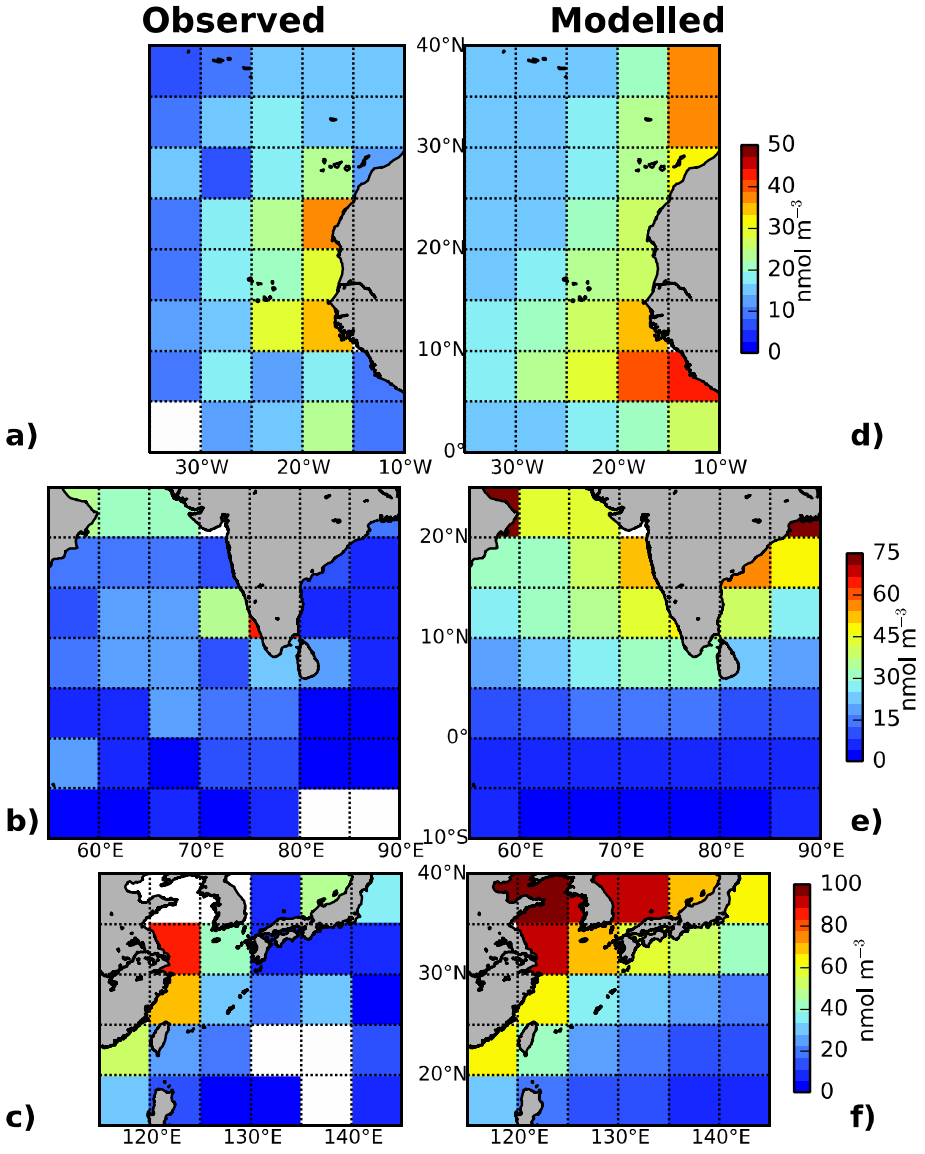

Fig. 5

Atmos. Chem. Phys. Discuss., doi:10.5194/acp-2016-1123, 2017
Manuscript under review for journal Atmos. Chem. Phys.
Published: 16 January 2017

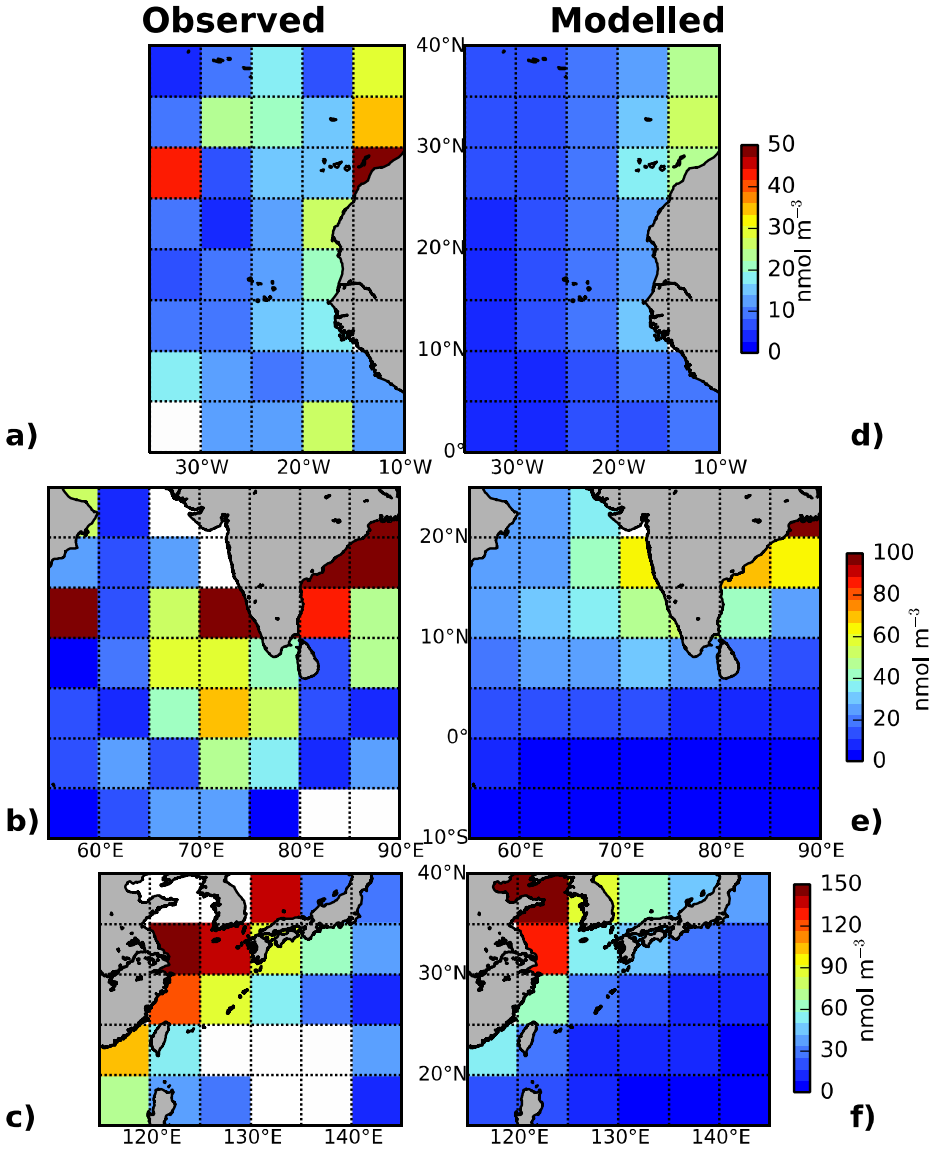

Fig. 6

Atmos. Chem. Phys. Discuss., doi:10.5194/acp-2016-1123, 2017
Manuscript under review for journal Atmos. Chem. Phys.
Published: 16 January 2017

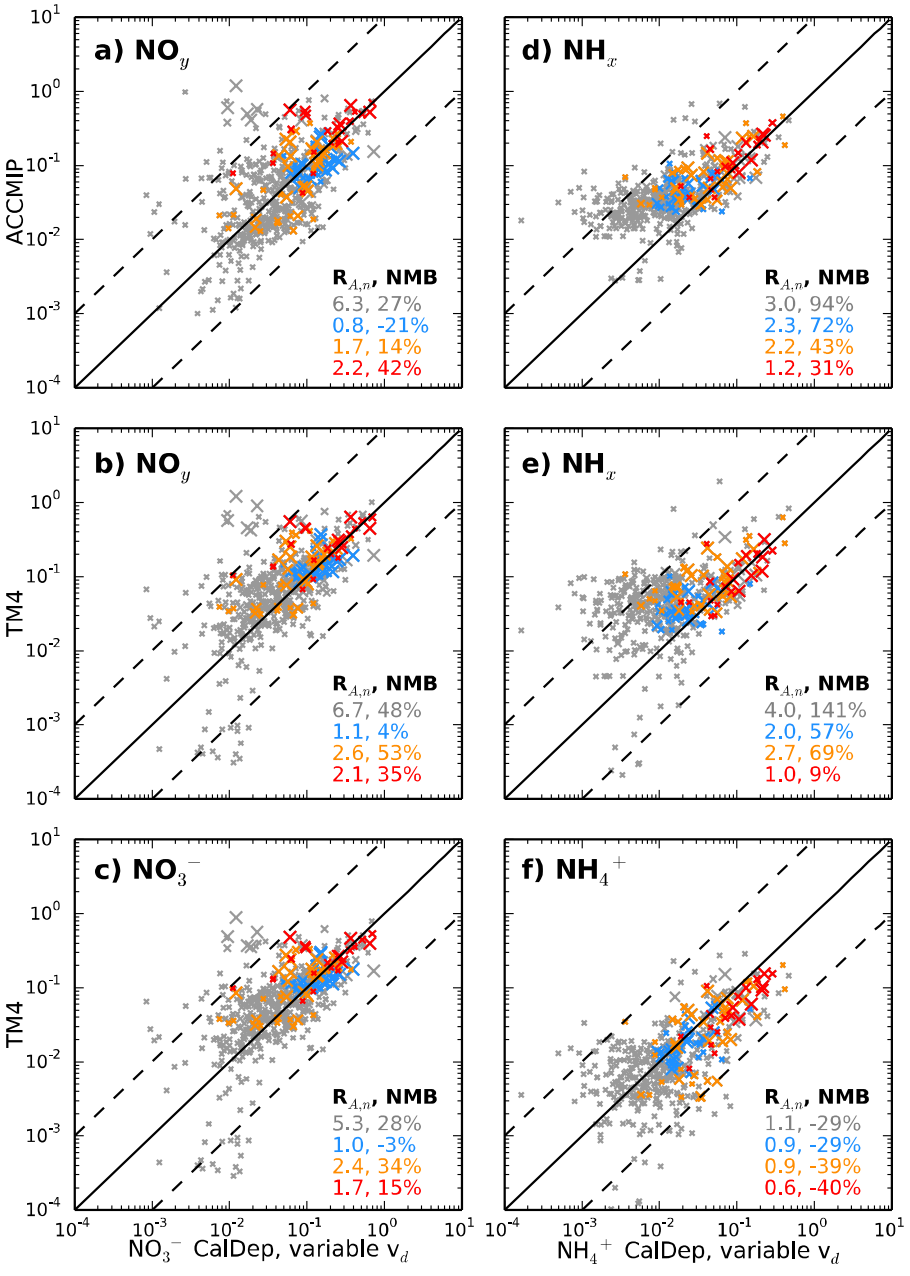

Fig. 7

Atmos. Chem. Phys. Discuss., doi:10.5194/acp-2016-1123, 2017
Manuscript under review for journal Atmos. Chem. Phys.
Published: 16 January 2017

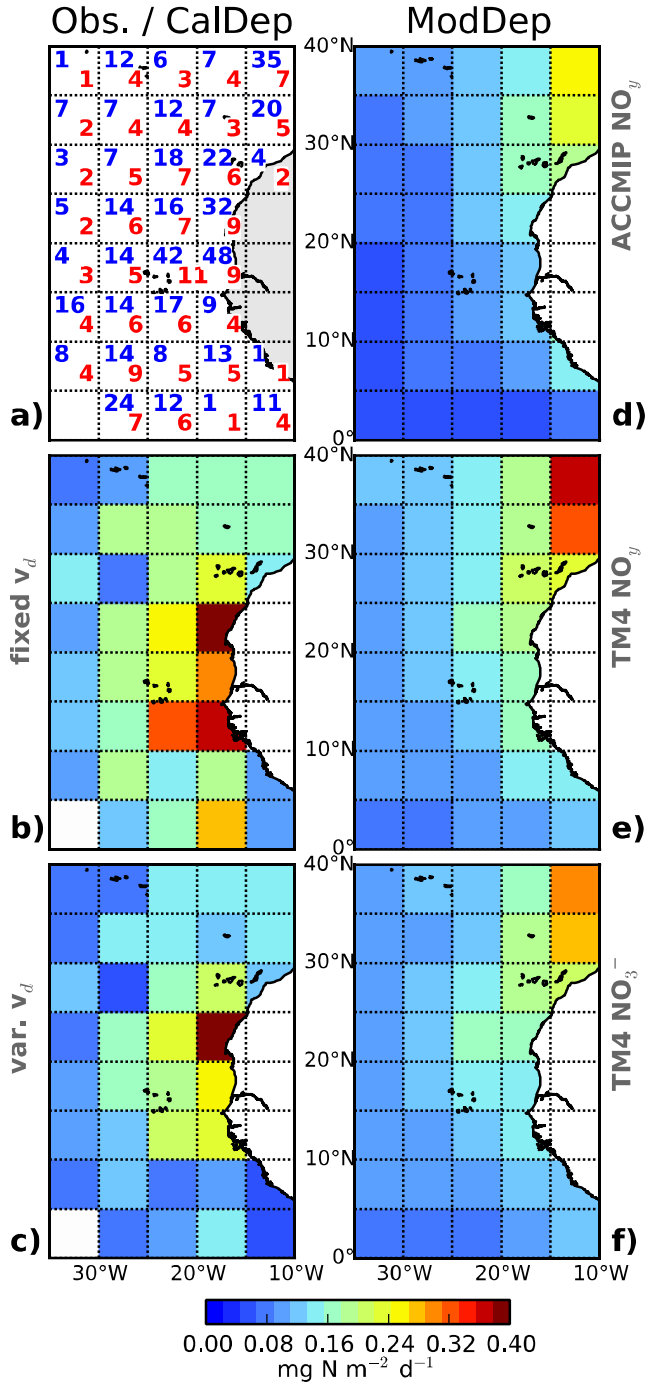

Fig. 8

Atmos. Chem. Phys. Discuss., doi:10.5194/acp-2016-1123, 2017
Manuscript under review for journal Atmos. Chem. Phys.
Published: 16 January 2017

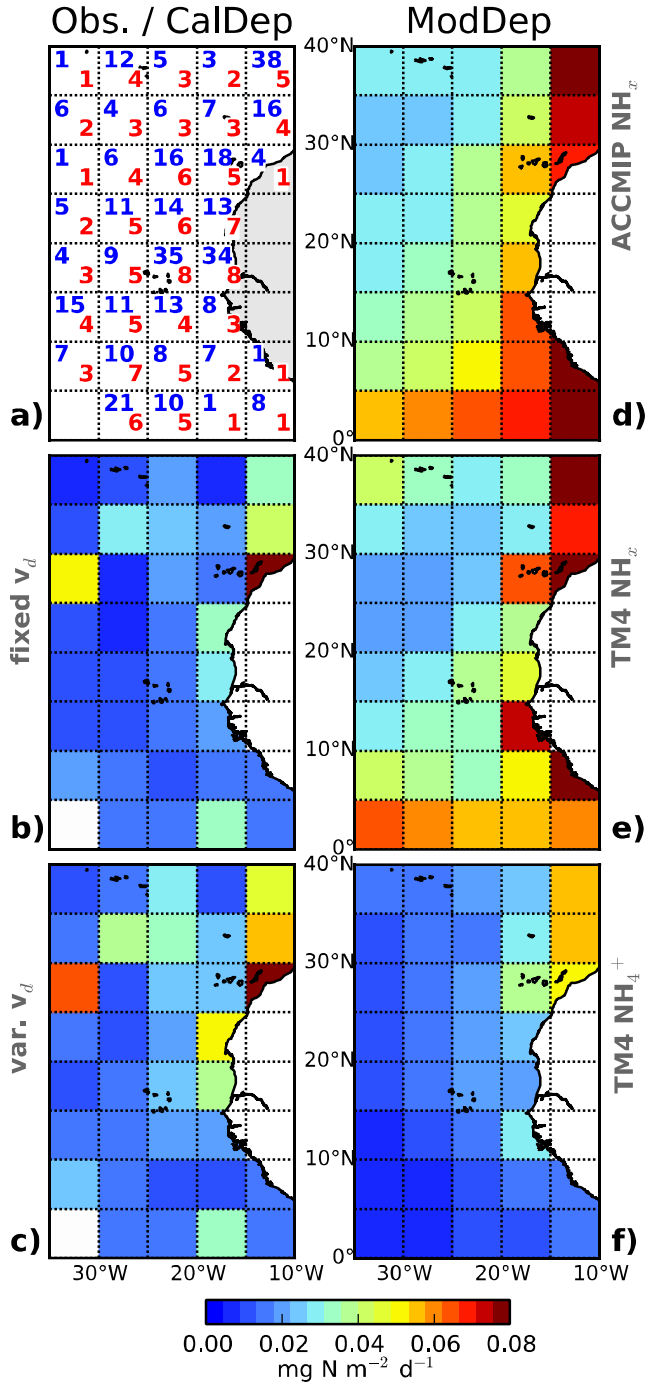

Fig. 9

Atmos. Chem. Phys. Discuss., doi:10.5194/acp-2016-1123, 2017
Manuscript under review for journal Atmos. Chem. Phys.
Published: 16 January 2017

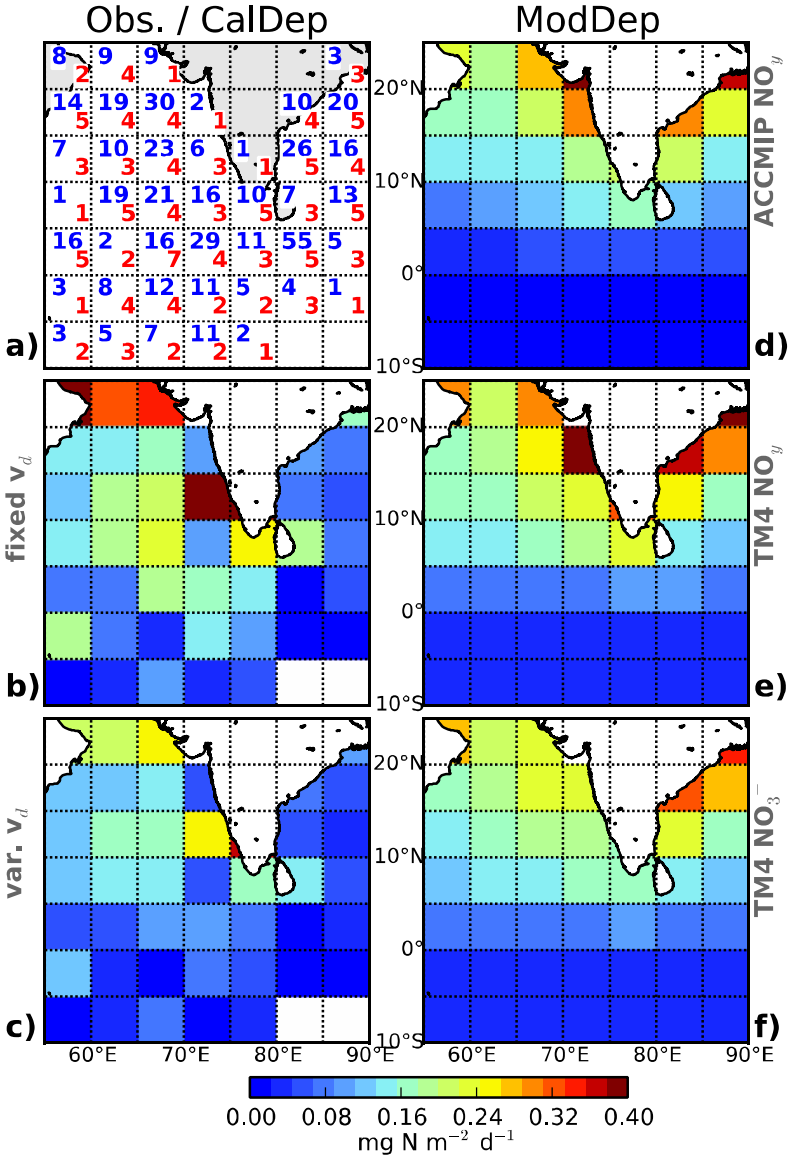

Fig. 10

Atmos. Chem. Phys. Discuss., doi:10.5194/acp-2016-1123, 2017
Manuscript under review for journal Atmos. Chem. Phys.
Published: 16 January 2017

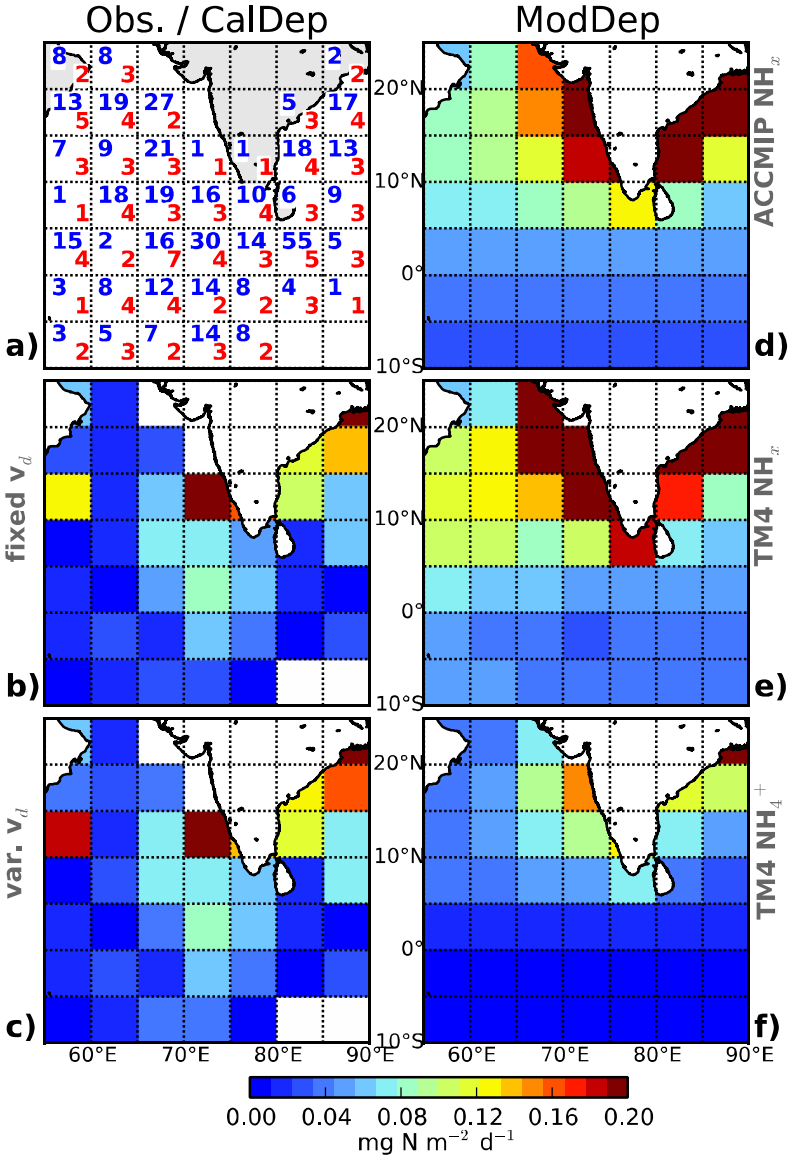

Fig. 11

Atmos. Chem. Phys. Discuss., doi:10.5194/acp-2016-1123, 2017
Manuscript under review for journal Atmos. Chem. Phys.
Published: 16 January 2017

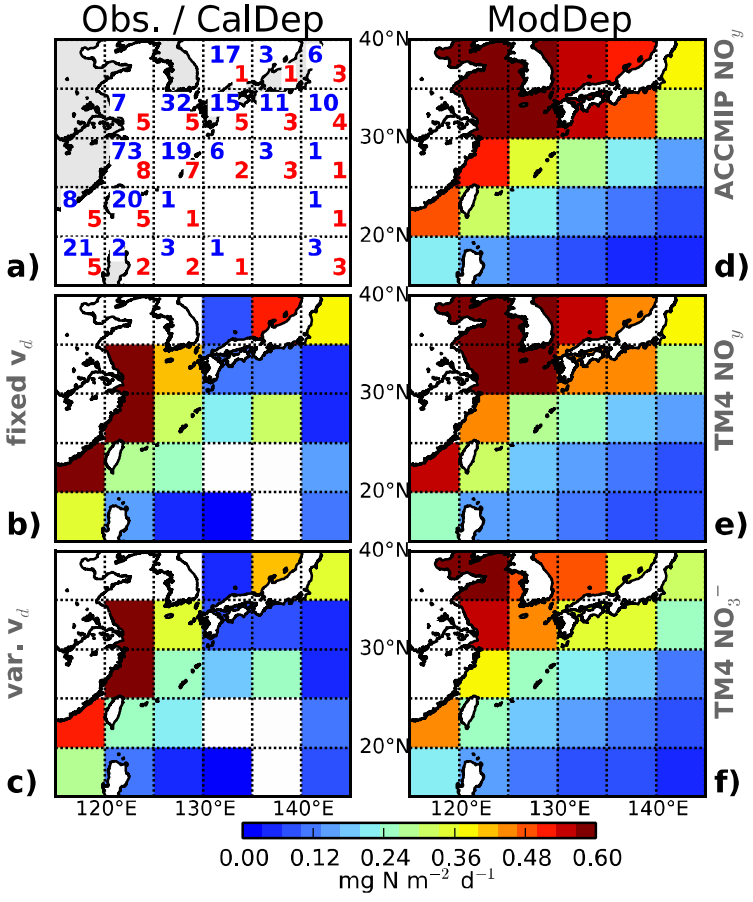

Fig. 12

Atmos. Chem. Phys. Discuss., doi:10.5194/acp-2016-1123, 2017
Manuscript under review for journal Atmos. Chem. Phys.
Published: 16 January 2017

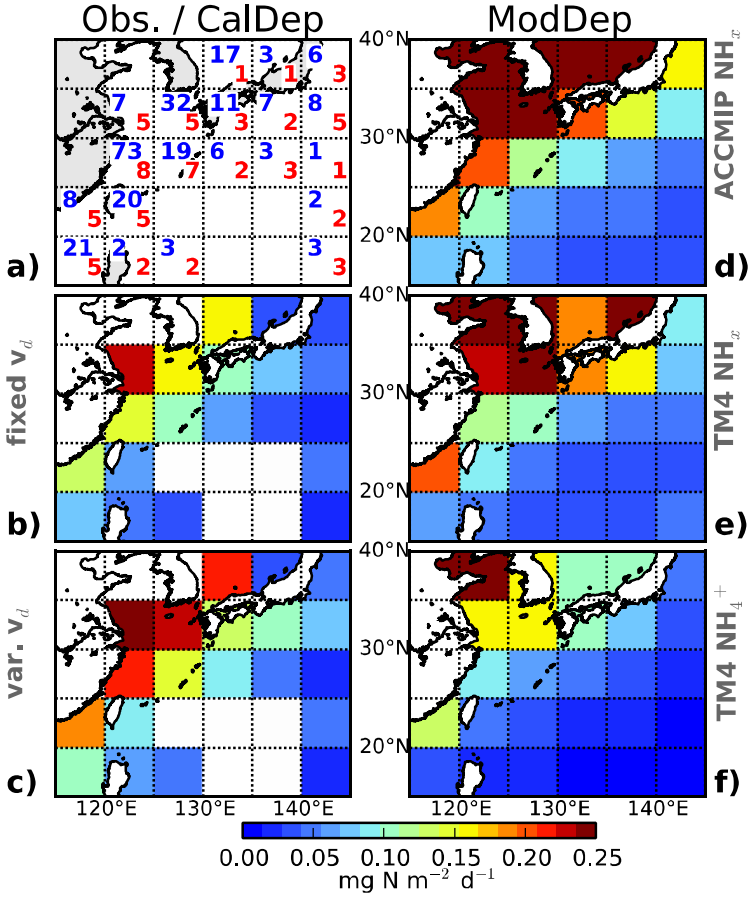

Fig. 13

Atmos. Chem. Phys. Discuss., doi:10.5194/acp-2016-1123, 2017
Manuscript under review for journal Atmos. Chem. Phys.
Published: 16 January 2017

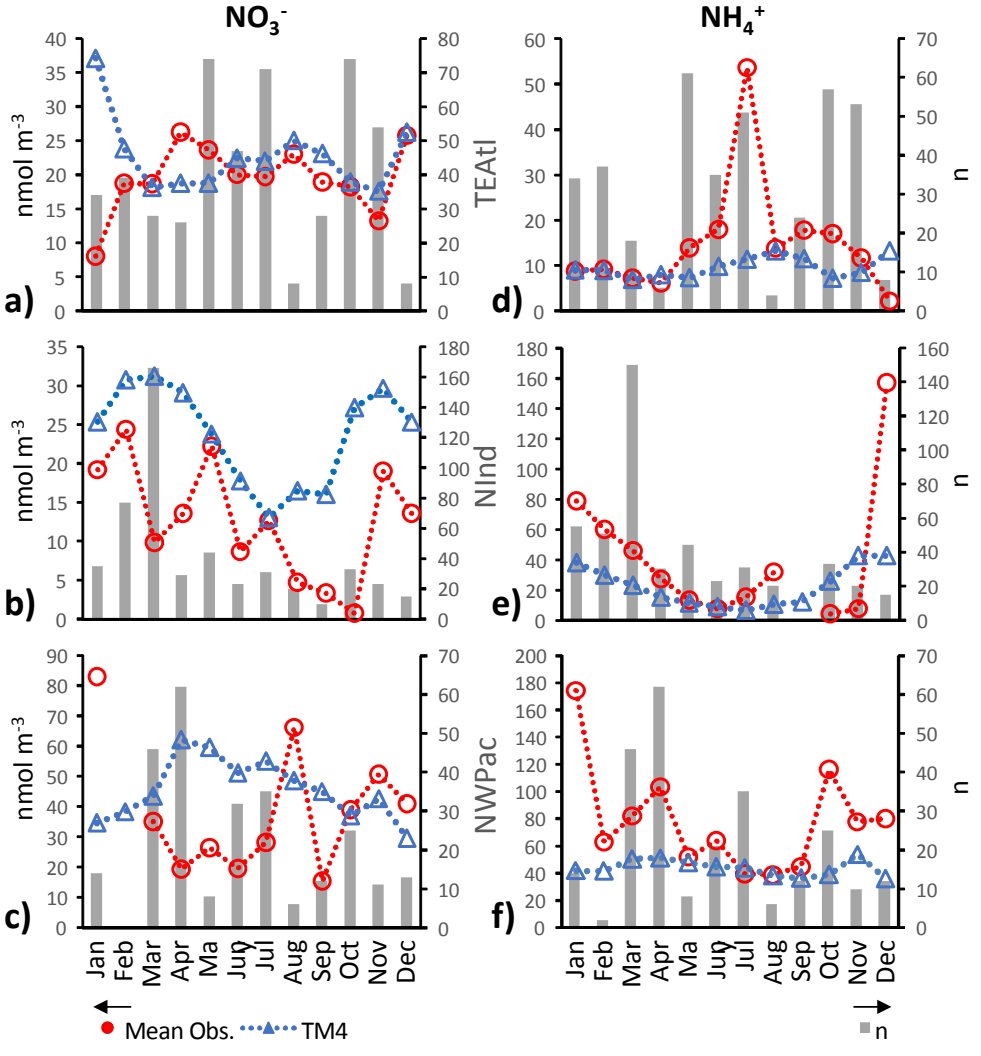

Fig. 14

Atmos. Chem. Phys. Discuss., doi:10.5194/acp-2016-1123, 2017
Manuscript under review for journal Atmos. Chem. Phys.
Published: 16 January 2017

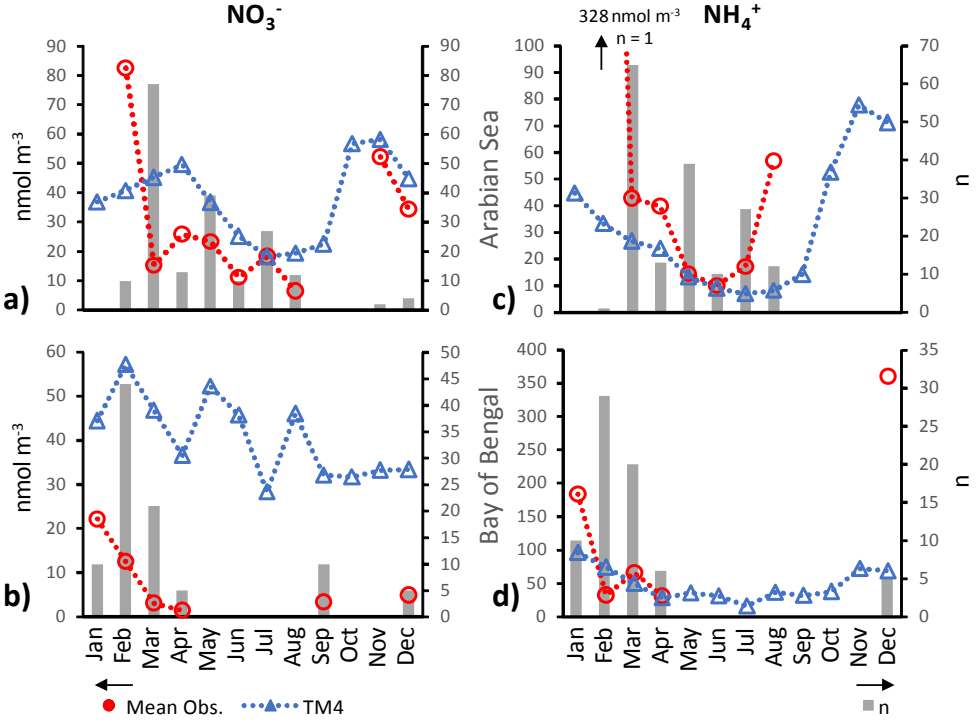

Fig. 15